University of Stavanger

Faculty of Science and Technology

MASTER'S THESIS

Study program/ Specialization: Petroleum Engineering - Master of Science Degree Programme	Spring semester, 2012. Open access
Writer: Steffen Helgesen Van der Veen	…… (Writer's signature)
Faculty supervisor: Merete V. Madland External supervisor(s):	
Titel of thesis: *Water induced compaction of chalks with varying non-carbonate content - The effect of Mg^{2+} and pH of the injected brines*	
Credits (ECTS): 30	
Key words: • Chalk • Harmignies • Lixhe • Water weakening • pH • Magnesium • Accelerating creep • Non-carbonate content	Pages: 60 + enclosure: N/A Stavanger, 8.6.2012 Date/year

Acknowledgments

I would like to express my gratitude towards Dr. Reidar I. Korsnes for his excellent guidance and assistance during all stages of writing this master thesis. I would also like to thank my faculty supervisor Assoc. Professor Merete V. Madland for insightful feedback throughout the process.

Stavanger, 8.6.2012
Steffen Van der Veen

Summary

The main objective for this study was to investigate the effect of alkaline brines on chalk, and the importance of non-carbonate content in chalk. This was done by flooding alkaline $MgCl_2$ on Liège chalk – which has non-carbonate content similar to that of North Sea Chalk, in addition to flooding the cleaner Mons chalk using $MgCl_2$ with normal pH (pH≈6). The tests were performed using a triaxial cell, heated to 130°C by a surrounding heating jacket. The chalk cores were initially put under hydrostatic pressure, where the confining pressure was being raised to a desired value (11-12 MPa) simultaneously with increasing piston pressure in axial direction. Prior to this phase, the cores had been flooded with NaCl and gained a pore pressure with a value of 0.7 MPa. After hydrostatic loading, the cores experienced a creep phase. Here, the confining pressure along with pore pressure and piston pressure were kept constant, and it was during this phase that the flooding brines were switched to the desired brines. The only source of discrepancy in creep compaction of the chalk cores was now the injection brine. During creep phase, water samples of the effluent brine were collected for analysis purposes. By doing this, information of what is being produced and retained in the chalk is gained, and one can get a better understanding of the chemical processes that is occurring during this phase.

Four different brines were flooded during these tests. NaCl was used as a pre-flooding brine for all five tests, and as a reference test for one of the Liège chalk cores. Alkaline 0.657 M NaCl and 0.0445 M $MgCl_2$ with equal ionic strength (pH value of 10 and 9.5 respectively) was flooded through Liège chalk cores to further examine the importance of magnesium, and the effect of alkaline flooding. 0.0445 M $MgCl_2$ was selected as this is the magnesium concentration to that found in seawater. 0.219 M $MgCl_2$ was flooded through the Mons core as a reference for the study of calcite purity effects.

During the hydrostatic phase, all four samples showed close to equal total axial strain, with values ranging from 1.05-1.10%. The Mons core seemed to be the strongest chalk with regards to yield strength; 9.9 MPa versus 8.6-9.10 MPa to that of the Liege cores.

During the creep phase, the Liège cores showed some interesting results. When switching from normal to alkaline NaCl, a slight deceleration in creep behavior was immediately observed compared to the reference core flooded with normal pH.

The alkaline 0.0445 M $MgCl_2$ flooded core showed close to equal strain rates of that flooded with alkaline NaCl during the first period of creep; 0.690 and 0.664%/decade respectively. However, after approximately 60 days of creep, the Mg flooded core showed an accelerated creep compaction. This behavior has been seen previously (Madland et al., 2011; Megawati et al., 2011), but at much higher magnesium concentrations (0.219M $MgCl_2$).

The results from the Mons core flooded with 0.219 M $MgCl_2$ indicated that magnesium ions were being retained inside the core along with excessive calcium being produced from the core, causing an enhanced creep compaction observed by an accompanying accelerating creep phase. The same was not seen during the accelerated creep phase for the Liège core. Although there was evidence of both magnesium being retained in the core along with calcium being produced, both the magnesium and calcium concentration seemed to flatten out, indicating that different processes might be occurring during this accelerated creep phase.

Table of contents

1 Introduction

The effect of aqueous chemistry on the mechanical strength of chalk has been thoroughly investigated during the last decade. When chalk is exposed to seawater at high temperatures (i.e. 130°C, which is the reservoir temperature to that of the Ekofisk Field in the North Sea), it has been proven that it is mechanically weaker than when exposed to distilled water, when considering the hydrostatic yield strength and the subsequent creep phase. The chemical processes occurring in the pore space has lately been described as the explanation for this discrepancy, as the rheological and physical characteristics of seawater and distilled water is quite equal. Water weakening of chalk has been a major issue for oil and gas producing companies ever since the discovery of seabed subsidence on the Ekofisk field in 1984. Even with the injection of seawater as a measure to sustain the reservoir pressure, the seabed subsidence has continued. The phenomenon is referred to as the water weakening effect on chalk. In the years following these events, major effort have been set to get an understanding of what is occurring down in the reservoir. Major research projects have been initiated, subsidized by both oil and gas companies and the Norwegian government, including several at the University of Stavanger.

In earlier years, the physical effects of the water weakening processes was granted most of the attention, as scientists concluded that the chemical effects was of minor importance. The strength of the chalk was believed to be controlled solely by the porosity and silica content (DaSilva et al., 1985). Flooding experiments done on outcrop chalk showed that the strength of the rock matrix was strongly dependent on the flooding fluid. The chalk was at its strongest when being completely dry, and a reduction in strength was seen when flooding with oil or glycol. It was also shown that the chalk was at its absolute weakest when flooded with water (Risnes, 2001). This lead scientists to believe that the water weakening effect could be controlled by different parameters in the fluid in which it was flooded.

Capillary forces were also believed to be of major importance when it came to the water weakening of chalk. Capillary forces are the physical forces interacting between fluids of different composition at the granular surface. It was believed that strong capillary forces were acting between water as a wetting phase, and oil/gas as a non-wetting phase. But experiments performed by Risnes et al. (2003) showed that cores saturated with glycol had much of the same strength as oil saturated cores. Glycol is

completely miscible with water, hence there should be no capillary forces interacting between the two fluids, and thus they concluded that capillary forces could not be the main driving mechanism behind the water weakening effect.

If the capillary forces were to be seen as negligible when discussing water weakening, there had to be some chemical aspects to the problem, especially since temperature seemed to be a factor to consider (Risnes, 2001). Korsnes (2007) proposed an ionic substitution process was taken place when chalk was being flooded with seawater at high temperatures. When the seawater contained sulphate ions (SO_4^{2-}) magnesium ions (Mg^{2+}) would substitute calcium ions (Ca^{2+}) at the grain surface. However, in-house tests performed by Madland et al. (2008) studied the water weakening of outcrop chalk from Kansas flooded with brines not containing any magnesium, and showed an even more enhanced water weakening effect even though no magnesium was present. Thus substitution cannot be the main driving mechanism in water weakening of chalk.

Even though substitution may not be the main driving mechanism, studies are still going on to determine what goes on inside the chalk when flooded with seawater. At the University of Stavanger, several tests are still being performed using different types of outcrop chalk and flooding with seawater (brines) with different composition under reservoir temperature and effective stresses. The purpose of flooding with different brines is to see how the chalk core reacts with different ions found in the seawater that are being injected into the reservoirs. The brines are composed of the elements in which we want to know how the chalk will react with. For example, if we wanted to know the effect of sodium chloride (NaCl) in seawater, one can flood the chalk plug using solely sodium chloride and water. An important issue when composing brines is to be aware of the ionic strength of the water injected. It is of essence that the all brines flooded through the chalk, are of the same ionic strength, so that this can be taken out of the equation when comparing the differences in the results. The ionic strength used to calculate the different amounts of ions desired in each brine is also quite equal to the ionic strength of the seawater injected in reservoirs.

Previous research has proven magnesium to be an important ion when considering the water weakening effect of chalk (Megawati et al., 2011; Madland et al., 2011),

hence the importance of magnesium was further investigated in this study. In addition, the importance of the purity of the chalk in relation to carbonate content and pH of the flooding brine was studied. This was done by performing tests on both highly pure outcrop chalk (Mons chalk from the quarry of Harmignies), and less pure chalk that has proven to be a good substitute for the reservoir chalk of the Ekofisk field (Liège chalk from the quarry of Lixhe)

The main objective for this study is to investigate the effect of alkaline brines on chalk, and the importance of non-carbonate content in chalk. This will be done by flooding alkaline $MgCl_2$ on Liège chalk – which has non-carbonate content similar to that of North Sea Chalk, in addition to flooding the cleaner Mons chalk using $MgCl_2$ with normal pH (pH≈6). The flooding will be performed under Ekofisk reservoir temperatures of 130°C and effective stresses.

2 Chalk

Chalk is defined as a sedimentary rock with over 90% of its content being calcium carbonate ($CaCO_3$). Chalk is formed by deposits of marine organisms and the skeletons of planktonic algae. One example of skeletons of planktonic algae is coccolith. The skeletons form a ring known as a coccolith ring. These are over the course of time mostly deformed, although some may stay intact, and form the chalk as we know it today. The chalk found in the North Sea is mainly built by intact skeletons or deformed skeletons of coccoliths. The intact rings have a dimension of 10 µm, while the deformed has a dimension of about 1 µm. Due to the unique structure of these coccolith skeletons, the chalk has a very special open structure. The pore space can even be found to exceed the size of the chalk grains, hence the high porosity (Risnes, 2001). The chalk and its pore space can be studied using a scanning electron microscope (SEM). With this one can see the immense pore spaces and structures. A SEM picture of an outcrop chalk from Liège in Belgium is presented in Fig. 2.1.

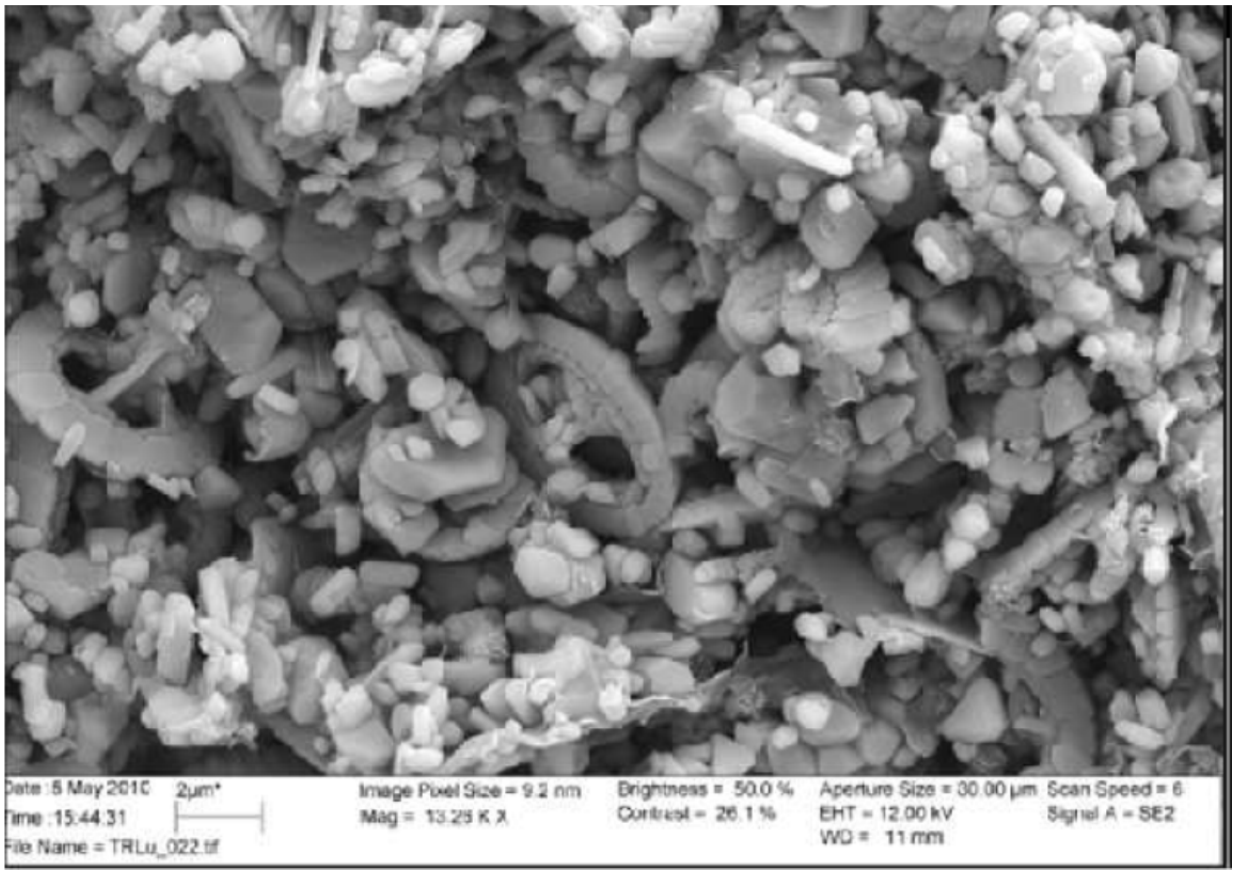

Figure 2.1: SEM Picture of outcrop chalk from Liège (Megawati et al., 2011).

3 Carbonate reservoirs

3.1 In general

Carbonates have proven to be a very important reservoir rock, and per today over half of our proven petroleum reserves are contained in carbonate reservoirs (Roehl and Choquette, 1985). Carbonate reservoirs contain mostly of calcite ($CaCO_3$) and dolomite ($CaMg(CO_3)_2$), and is subdivided in two groups; limestone and dolomite. The calcite in limestone is mostly the product of marine organisms. Pure dolomite contains 90% or more dolomite, and pure limestone contains 90% or more calcite. The carbonate reservoirs worldwide are divided into 50% limestone and 50% dolomite (Zenger et al., 1980). Pure limestone reservoirs have a low porosity, ranging from 2-20% but the permeability can range from 0-100 millidarcy (mD) depending on the fracture system inside the reservoir. Dolomite reservoirs have a lower range of both porosity and permeability (Schmoker et al.,1985).

Chalk is a very important reservoir rock in the southern part of the North Sea, and is defined as a limestone that has kept its biogenetic origin maintained. Chalk reservoirs in the North Sea have kept a very high measure of porosity, scaling up to almost 50% with a permeability ranging from 1-5 mD. The strength of chalk generally decreases with increasing porosity and increases with increasing silica content. Weak chalks contain porosities higher than 35% and have silica content less than 5-7% (DaSilva et al., 1985)

The production of petroleum resources from carbonate reservoirs are divided in three phases. The first phase of production is natural pressure depletion, as most of the carbonate reservoirs in the North Sea are overpressure, naturally fractured high porosity reservoirs (Sylte et al., 1999). During this phase, only 5-30% of the original oil in place is produced (Farouq-Ali and Stahl, 1970). Over time while producing, the energy stored in the reservoir will gradually decrease, which necessitates further means for economically efficient production, known as the secondary phase. Examples of means initiated in the secondary phase of production, can be injection of water, gas or both (WAG – water alternating gas injection). The tertiary production period is the last stage in the production cycle. Miscible gas flooding, chemical

flooding, thermal methods or a combination of these methods are techniques used in this stage.

Fractures in the rock matrix and its wettability are important factors for oil recovery from carbonate reservoirs. As mentioned, carbonate reservoirs have a low permeability, which makes the existence of natural fractures in the matrix very important when producing oil as most of the oil is stored in the rock matrix. The main challenge when producing is to get the oil from the rock matrix into the fracture network. This is challenged by the wetting state of the rock. Over 90% of the carbonate reservoirs are neutral to oil wet (Downs and Hoover, 1989), so when injecting water into the matrix, the water is likely to follow the fracture system to the production well, bypassing and leaving behind most of the oil.

As rock samples from the reservoirs are scarce, outcrop chalk has been used as an analogue to reservoir chalk. As chalk compositions vary with geographical position, finding the perfect outcrop chalk has been proven to be very difficult. In Fig. 3.1, non-carbonate content of outcrop chalk types are compared to the reservoir chalk of the Valhall field. As seen from the figure, the reservoir chalk contains minerals that are not present in the outcrop chalk (e.g. Kaolinite). These minerals may also have an impact when it comes to the water weakening effect. What is of interest to note is that the total percentage of non carbonates found in Liège chalk (represented as Hallembaye in Fig. 3.1) is of similar values as that found offshore, ranging from 1-3%, with nearly equal values of quartz content.

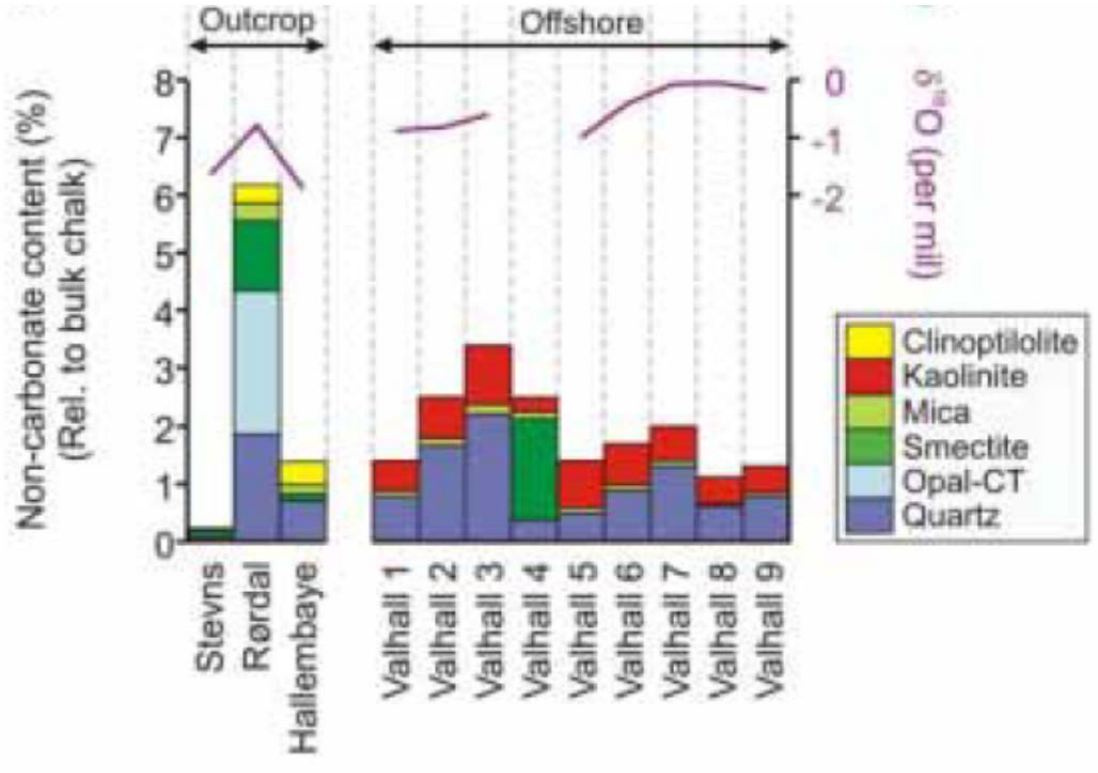

Figure 3.1: *Quantity relations between non carbonate content and calcite on outcrop chalk and core samples collected from the Valhall field (Hjuler, 2006).*

3.2 The Ekofisk field

The Ekofisk field is located in the central graben in the southern part of the Norwegian sector of the North Sea. Early production started in 1971 with oil expansion, solution gas drive, reservoir compaction, and limited natural gas injection as the primary drive mechanisms, until water flooding started in 1987 (Madland, 2005). It was during this phase the problem of water weakening was discovered.

When pressure depletes from the reservoir, the depletion may lead to compaction in weak formations. There is an immense weight of overlying rock, and as the pressure drops, the rock matrix may give in and collapse. This is what happened in the Ekofisk field, and as a result of this there was a noticeable change in sea level on the platform; the seabed had actually subsided several meters. Seabed subsidence was not at all expected, but was discovered in 1984. As a result of this discovery, it was suggested that reservoir compaction was a more important mechanism in the production of hydrocarbons than first anticipated; as of 2008 9 meters of seabed subsidence has occurred at the Ekofisk field since the start of production with a rate of calculated to be

about 0.4 meter per year (Spencer et al., 2008). This seabed subsidence is well noticed in Fig. 3.2, which displays a photograph of one of the platforms on the Ekofisk field (2/4 T) that has been lifted after seabed subsidence. The previous water level can be noticed by the darkened area on the concrete foundation. These circles were also how seabed subsidence was discovered in the first place, as a mere coincident when one of the workers on board a neighboring platform counted the circles and compared them with a picture of the platform from when it was just installed.

After 16 years of production, water injection was initiated. Improved oil recovery as a result of injecting seawater has been a great success, with an expected oil recovery reaching 50%. With the injection of seawater, the reservoir pressure was kept constant, or even slightly increased, during production but compaction and subsidence is still a problem due to water weakening of chalk.

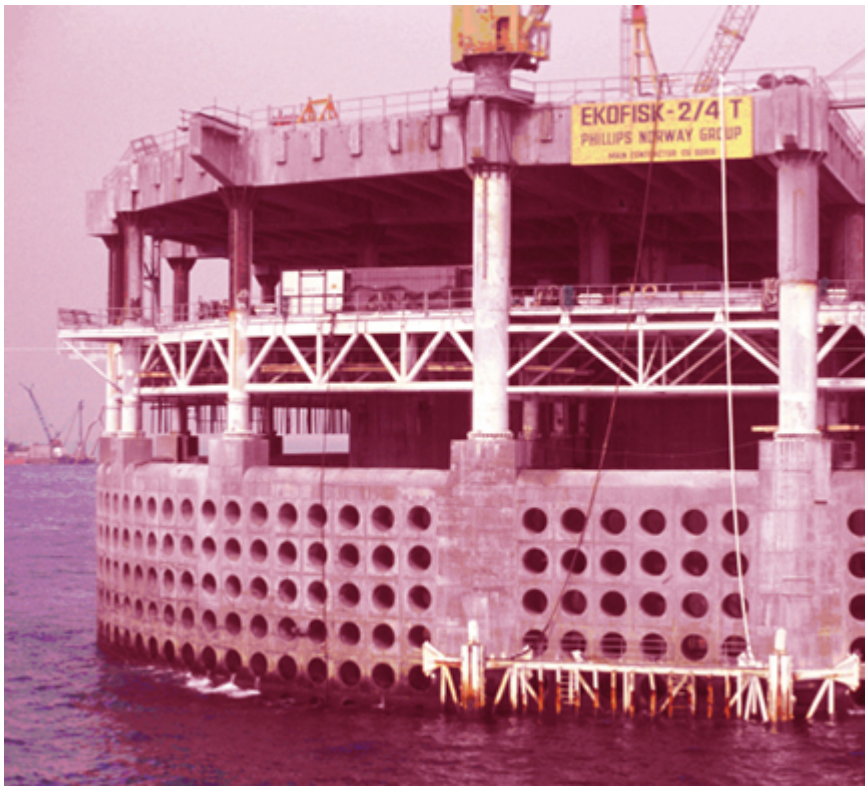

Figure 3.2: *Photograph of Ekofisk – 2/4T after it had been lifted to account for the seabed subsidence (from www.npd.no).*

4 Mechanical properties

The following definitions and theories are based on the book “Petroleum related rock mechanics” (Fjær et al., 1991)

4.1 Stress

Stress, σ, is a measure of the average amount of force exerted per unit area (A) of a surface within a deformable body on which internal forces (F) act. In the SI-system, stress is measured in Pascal [Pa], which is equivalent to Newton per square meters [N/m^2]. As a notation, the Greek letter sigma is used:

$$\sigma = \frac{F}{A} \tag{4.1}$$

Stress is not uniformly distributed over a cross section of a material body. Therefore the stress must be measured at a point on a given area, which will be different than the average stress. Looking at a cylinder, forces can be exerted in either axial or radial direction, Fig. 4.1

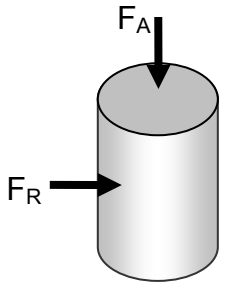

Figure 4.1: *Axial and radial forces exerted on the surface of a cylinder*

4.1.1 Axial stress

Axial stress, σ_A, is defined as

$$\sigma_A = \frac{F_A}{\pi r^2} \tag{4.2}$$

where F_A is the axial forces exerted to the cylinder with a radius r.

4.2 Strain

Strain, the deformation a material undergoes as a result of stress, can be elastic, whereas the material has the ability to return to its original state, or plastic, whereas the forces exerted has exceeded the internal forces of the material resulting in an irreversible deformation known as yield.

4.2.1 Axial strain

Axial strain, ε_A, is defined as

$$\varepsilon_A = \frac{L - L'}{L} \tag{4.3}$$

where L is the length of the cylinder at original state and L' is the length of the cylinder when deformed (see Fig. 4.2).

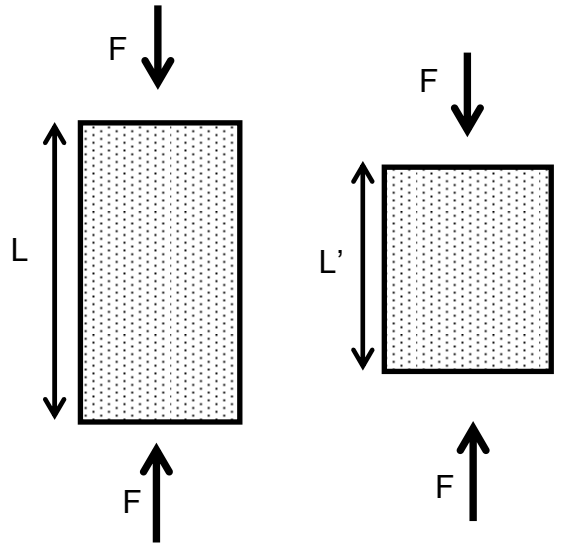

Figure 4.2: *Axial stress deformation due to axial force F.*

4.3 Stress-Strain relation

For a linear elastic material, there is always a constant relation between stress and strain. This relation for an elastic material is given by a straight linear line. When the stress level exceeds the internal forces within the material, the curve will crack and start to decelerate, in other words go from elastic to plastic state, Fig. 4.3.

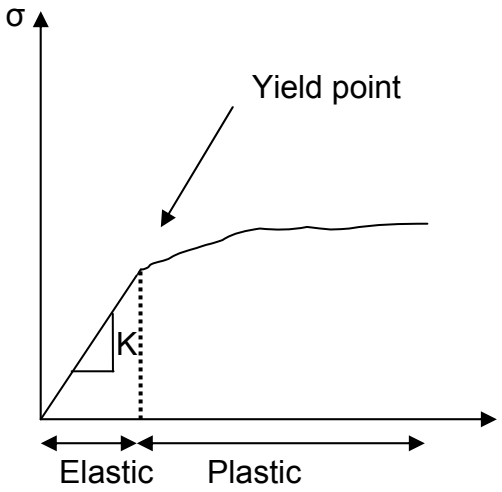

Figure 4.3: *Stress – Strain relation. After the material has reached yield point, there is no return to the original state.*

Chalk behaves as a frictional material, failing in shear failure mode. The rock matrix of chalk has an open structure that enhances a failure system referred to as pore collapse (Blanton, 1981).This is an important failure mechanism as the chalk grains may be smaller than the pore space. This allows the chalk grains to be forced into the pore space. The pore collapse mechanism has therefore in some cases, been referred to as an implosion of the material. These events can take place under hydrostatic conditions, even though there are no shear stresses present at a macroscopic scale (Fjær et al., 1991). On the microscopic scale, the individual grains can experience shear stresses, and pore collapse may therefore be regarded as distributed shear failure within the material.

The K-module is the elastic coefficient used to determine the relation between stress and volumetric strain under hydrostatic conditions. It values how much a material will be compressed when exerted a certain amount of stress.

The K-module can be defined as:

$$K = \frac{\sigma_h}{\varepsilon_v} \qquad (4.4)$$

where $\sigma_h = \sigma_x, = \sigma_y = \sigma_z$ equals the hydrostatic stress.

The volumetric strain defined as total strain from all directions:

$$\varepsilon_v = \varepsilon_x + \varepsilon_y + \varepsilon_z \quad (4.5)$$

During hydrostatic conditions, the strength of the material can be assumed isotropic.

$$\varepsilon_V = 3\varepsilon_A \quad (4.6)$$

The inverse K-module, 1/K is known as the compressibility factor (C).

4.4 Creep

One way to measure the water weakening effect on chalk is to measure the creep. Creep is defined as the time dependent deformation that occurs when a material is under constant stress at a constant temperature. It can be subdivided into three stages: Transient, steady state and accelerating shown in Fig. 4.4.

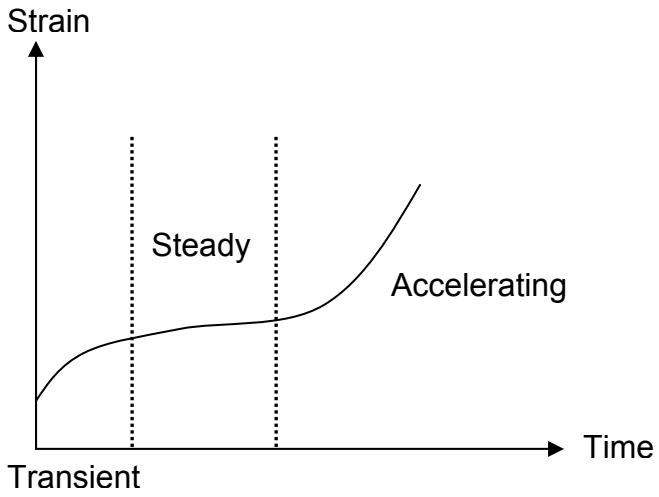

Figure 4.4: *Strain versus time for a material under creep conditions.*

As seen from Fig. 4.4, during the transient creep, deformation rate decreases with time until it reaches a more steady and linear period; the steady state. During this state the material experiences constant and permanent deformation. The rate of deformation may increase through the elapse of time, and this state is referred to as the accelerating state. During this state, in a deviatoric test, the deformation is so immense that it will fail rapidly, and the process may be associated with a rapid spreading of unstable fractures. In a hydrostatic test, the isotropic pressure will prevent the chalk to fail rapidly.

From the comparison of the creep curve given by different chalk cores saturated with different compositions of brines, we can determine how the chalk reacts with the different ions present in the brine. By repeatedly collecting water samples during the test, we can determine the concentration of the ions present in the brine at given times during the test. This can then be compared to the creep to see if there are relationships between total creep and concentration of certain ions. With this we can get an understanding of the chemical reactions that occur down in the reservoir when flooded with seawater.

A measurement of how strain develops with time is the strain rate, m, also called strain per decade. This can be measured using a creep plot where axial strain is plotted as a function of logarithmic time. A linear line can be drawn where the creep reaches a linear trend in the logarithmic plot and strain rate, m, can be calculated using the following equation:

$$m = \frac{\Delta \varepsilon_C}{\Delta \log t} \tag{4.7}$$

where ε_C = creep strain [%] and t = creep time [days]

5 Water weakening of chalk

5.1 General

Chalk is a highly porous rock, which results to the mechanical strength of the rock itself being a function of the porosity. With such a high porosity, chalk is extremely sensitive to the type of fluid (brine) filling the pores. The mechanical properties of the rock changes as the saturation level increases. This includes hydrostatic yield stress, which is reduced by almost a factor of two compared to a dry rock (Fig. 5.1).

It is also proven, that dry chalk is not really dry. If heated above the normal drying temperature (100°C -110°C) additional water is being evaporated from the chalk, resulting in additional gain in strength. Also, it has been shown, that very little water is needed to activate the water weakening effect (Schroeder et al., 1998; Lord et al., 1998; Madland et al., 1999)

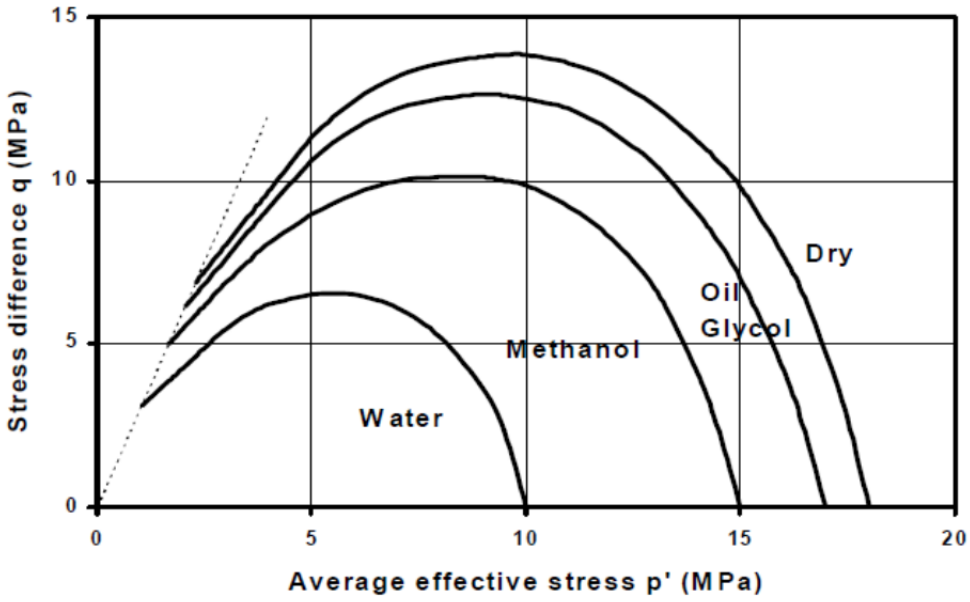

Figure 5.1: *Typical yield curves for different fluids (Madland, 2005).*

5.2 Chemical water weakening of chalk

The chemical weakening effect of water injection in chalk has not been granted as much attention as the capillary forces, but some studies have proposed chemical processes such as grain to grain dissolution, pressure dissolution, precipitation and re-crystallization when considering water weakening of chalk. The reason why chemical effects have been more or less disregarded is probably due to the very low solubility of $CaCO_3$ in pure water.

When injecting a fluid in a non-chemical equilibrium with the contact material, chemical reactions may occur. One of these reactions can be dissolution of various components which then again can react chemically with one another and precipitate. This dissolution-precipitation reaction can contribute to compaction of the reservoir, as the chalk is being dissolved. Experiments performed by Newman (1983) on oil saturated cores under stress, showed that injection of brines in chemical equilibrium with the rock did not lead to compaction, while injection of non-equilibrium brine lead to instant compaction. He concluded that the dissolution of the calcium carbonate in the chalk lead to compaction and mechanical failure at low stresses, while pressure solution occurred together with dissolution at high stresses.

Another important factor when analyzing chemical reactions is temperature. It is widely known that with an increase of temperature, the chemical reaction process increases linearly. As a rule of thumb we can assume that the speed of the reaction will double for each 10°C increase in temperature. Korsnes et al. (2006a and 2006b) did work on the temperature effect on the weakening of chalk by seawater, and concluded its importance. Temperature played an important part in the proposed Mg^{2+}/Ca^{2+} substitution process. The reduction in mechanical strength at increased temperatures was proposed to be the result of the substitution of Ca^{2+} by Mg^{2+} at inter granular contacts in the presence of SO_4^{2-} (Fig. 5.2). Temperature also plays an important role in the chemical dissolution of chalk. This can be seen as another water weakening mechanism, where this process increases with decreasing temperature as shown in Fig. 5.3, and the temperature effect on this process is the opposite of the former mechanisms.

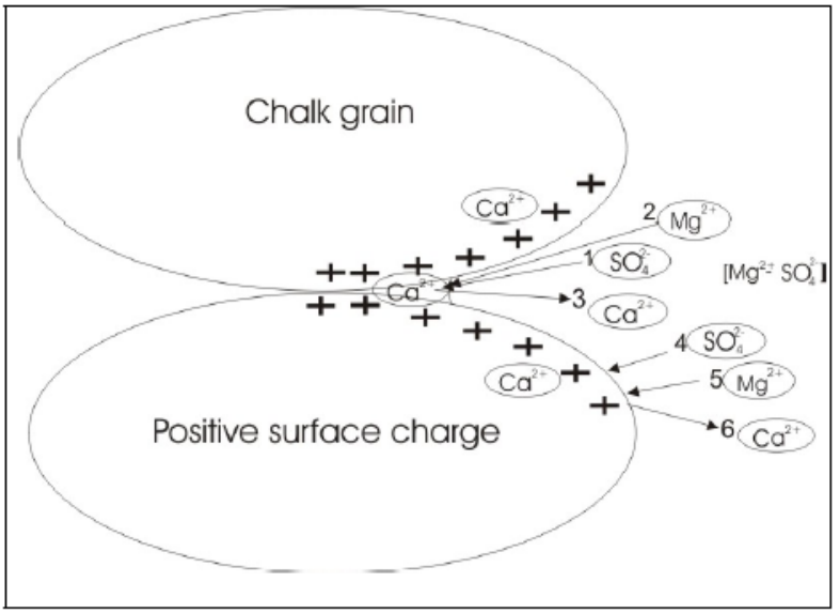

Figure 5.2: *Suggested mechanism of enhanced water weakening in chalk (Korsnes, 2007).*

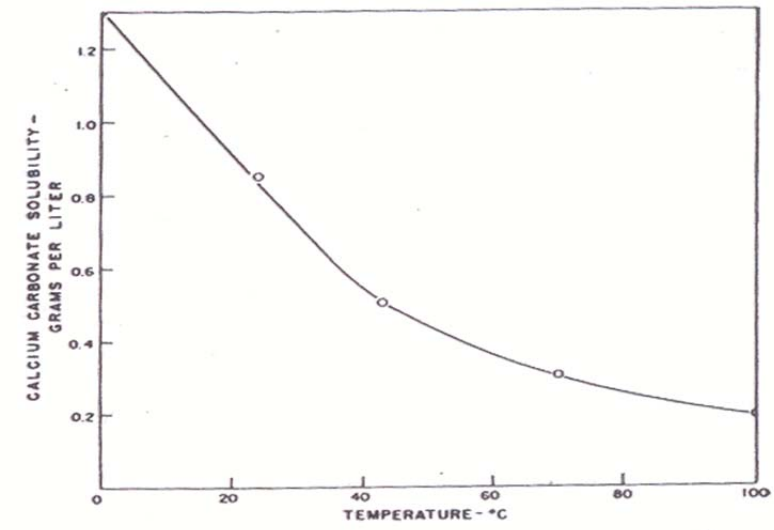

Figure 5.3: *Chemical dissolution of chalk. Temperature effect on the solubility of $CaCO_3$ in pure water at 0.987 atm. CO_2 pressure (from Miller 1952). Note that the process increase with decreasing temperature (Madland, 2005).*

Recent studies has investigated the weakening effect of more simple brines, such as pure sodium chloride with water (NaCl) and magnesium chloride ($MgCl_2$) with water. This has been done to investigate the specific effect of each ion. When flooding with $MgCl_2$ dissolution-precipitation processes seem to take place (Madland et. al., 2011). A significant amount of magnesium is being lost inside the core along with calcium

being produced. When the total calcium- and magnesium concentration was added in the sample effluent brine, the level stayed close to the original concentration of magnesium injected. The proposed reason for this was a substitution process combined with dissolution and precipitation of magnesium bearing minerals inside the core, as the results showed that there seemed to be a one to one exchange of magnesium and calcium.

These tests were performed on Liège chalk and Stevns Klint chalk. For the Liege chalk, when flooding with $MgCl_2$ the rock was mechanically weaker compared to NaCl during creep phase. The opposite was seen in the beginning when flooding Stevns Klint chalk with the same brine, but this process accelerated and reached the same values of deformation during creep phase as experienced on the Liège chalk.

5.3 The effect of pH

Previous studies performed by Megawati et al. (2011) shows a correlation between the change in pH on the flooding brine and the resulting creep deformation. It is well established that calcite ($CaCO_3$) is acid soluble, hence it was expected that chalk would experience a dependence of creep compaction with decreasing pH. However, their results showed that by injecting alkaline $MgCl_2$ solutions (pH>7) an enhanced creep compaction was observed.

6 Material and methods of work

6.1 Test material

High porosity outcrop chalk was used in the experimental work. Chalk formations exist today on the surface many places in Europe. This provides us with an opportunity of finding chalk outcrops with similar properties as the chalk formations found in the North Sea. Chalk material retrieved from reservoirs is usually very limited, however outcrops collected from surface chalk formations work as a substitute as they are available in large quantities. In these experiments, outcrop chalk from the quarry of Lixhe near Liège, and from the quarry of Harmignies near Mons, both in Belgium, has been used. Chalk information is listed in Table 6.1.

Table 6.1: *Outcrop chalk properties*

Outcrop chalk	Quarry	Age	Porosity approximation	Calcite content	Permeability
Mons	Harmignies, Belgium	Campanian	41-44%	99.4%	2-4mD
Liège	Lixhe, Belgium	Campanian	40-43%	94.7%	1-2mD

Chalk from Liège has been known to be a good substitute for reservoir chalk in the North Sea. The carbonate content of that in the outcrop chalk from Liège is quite similar to that found in carbonate reservoirs in the North Sea, e.g. the Ekofisk Field, both with values ranging from 4-5% (Hjuler & Fabricius, 2009).

As of date, there are little to no published information regarding the mechanical strength on Mons chalk, hence little is known about the mechanical properties of this outcrop chalk. In Richard et al. (2005), the porosity of Mons chalk was recorded to be in the vicinity of approximately 40-43%, and in Richard and Sizun (2011), the permeability was recorded to be in the range from 2mD to 4mD. Recent in-house studies have shown that Mons chalk is a highly pure chalk with respect to carbonate content; containing 99.4% calcite.

6.2 Preparation

The test material was extracted from the chalk blocks retrieved from Belgium. In order to make the chalk fit in the triaxial cell, the chalk cores were drilled from the outcrop block, shaped with a lathe and cut into the right length. The chalk cores were placed in a heating cabinet for drying at 90^{O}C. When the chalk was properly dry, which usually takes 24 hours, dry weight was measured before the plugs were saturated with distillated water in a vacuum chamber for porosity measurement. During preparation different core properties were registered, this information is listed in Table 6.2.

Table 6.2: *Chalk plug information from the chalk cores used in the experiments*

Chalk core	Length [mm]	Diameter [mm]	Dry weight [g]	Saturated weight [g]	Bulk Volume [ml]	Pore Volume [ml]	Porosity [%]
LS7	71.0	37.0	118.9	150.8	76.3	31.9	41.8
LS8	70.1	37.0	116.2	148.4	75.5	32.2	42.6
LS9	70.1	37.0	115.0	147.5	75.3	32.5	43.1
MS4	70.5	37.0	114.5	147.3	75.8	32.8	43.3

6.3 Test equipment

6.3.1 Triaxial Cell

Four mechanical tests were performed using a hydraulically operated triaxial cell, see Fig. 6.1). This is a high pressure, high temperature (HPHT) cell, allowing for testing at reservoir conditions.

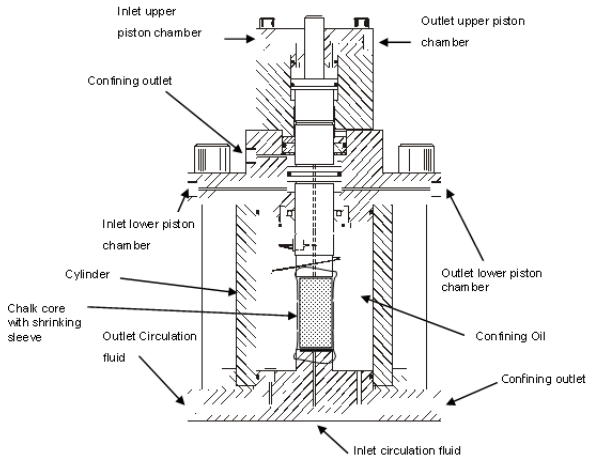

Figure 6.1: *A standard triaxial cell (Vorland, 2004).*

6.3.2 High pressure pumps

The triaxial cell was operated by two high pressured Quizix QX pumps as shown in Fig. 6.2; controlling confining pressure and axial pressure, and a high pressure Gilson pump controlling the fluid circulation. These pumps are controlled by a computer, which also shows real time graphs of measured data for test control purposes in the software Labview.

Figure 6.2: *High pressure Quizix QX pumps controlling the piston (axial) pressure and confining pressure.*

6.3.3 Heating system

The tests were performed under Ekofisk field temperature (130^{o}C). To keep this temperature during the test, a Backer 1500W heating jacket was placed around the cell (see Fig. 6.3), regulated by an external Omron HJCU-COM heat jacket control unit to raise the temperature to the desired level, and regulate for any temperature fluctuations in the surroundings throughout the test.

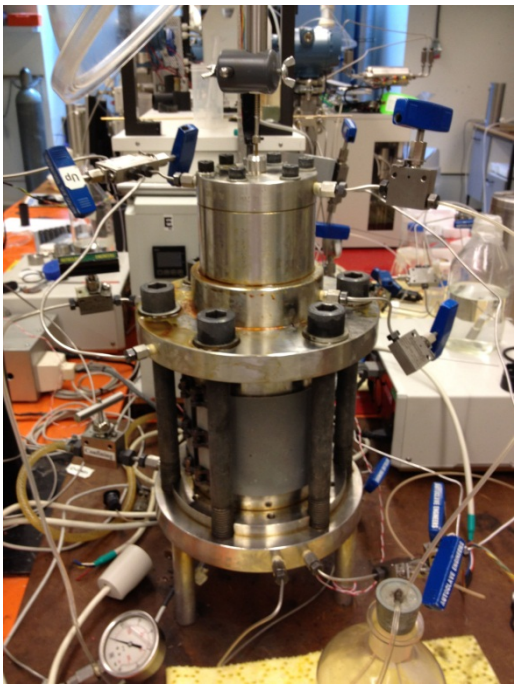

Figure 6.3: *Triaxial cell during testing, complete with heating jacket.*

6.3.4 Chemical testing

All water samples were chemically analyzed to measure the different anion and cation concentration. This was done using a Dionex ICS-3000 ion chromatograph (see Fig. 6.4). Before the water samples could be analyzed in the ion chromatograph (IC) they had to be diluted with distilled water and filtrated. The water samples were diluted 500 times using a Gilson Gx-271 diluter (see Fig. 6.5) and filtrated using syringes and syringe filters. All effluent water samples was also pH tested, using a SevenEasy METTLER TOLEDO pH meter (see Fig. 6.6)

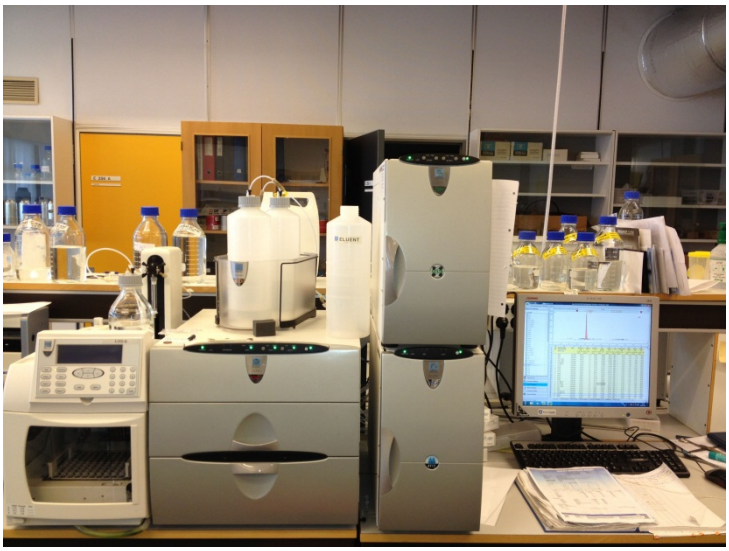

Figure 6.4: *Dionex ICS-3000 Ion Chromatograph used for chemical analysis of the effluent brine.*

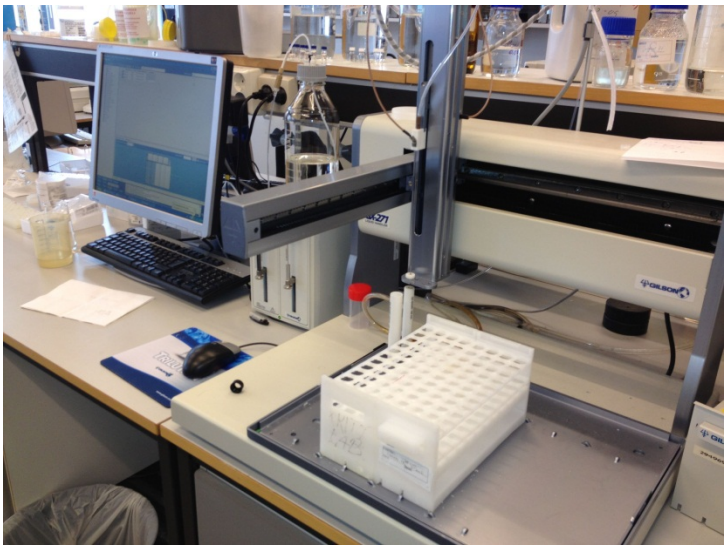

Figure 6.5: *Gilson Gx-721 diluter, used for diluting the effluent brine samples prior to chemical analysis.*

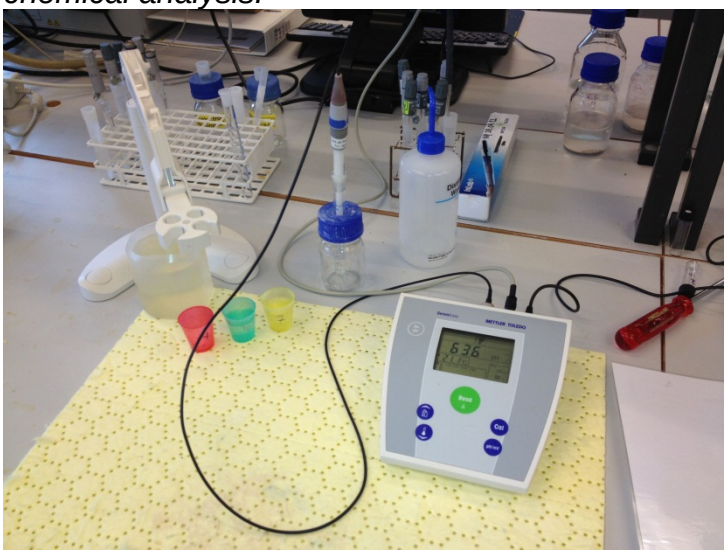

Figure 6.6: *SevenEasy METTLER TOLEDO, used for measuring the pH of the samples.*

6.4 Procedure

One test consists of two phases, the first one being a hydrostatic test where the radial and axial stress is increased simultaneously up to a pre-set stress level. The next phase is a creep phase where the stress is kept constant. This is done by keeping the confining pressure constant, in this case at 11 MPa for the Liège chalk cores, and 12 MPa for the Mons chalk core. During these phases the core is flooded with brine at a rate of 1 pore volume per day (1PV/day). To flood the circulation fluid (brine) a flooding cell is used. It contains 2 chambers which are separated by a piston. By flooding distilled water in the upper chamber, the piston is forced downwards and thereby pressing the brine through the chalk core.

The chalk core was placed in a shrinking sleeve and heated using an industrial heater (see Fig. 6.1). This was done to make sure that no leakage was possible. After fitting the chalk core on the cell base, the cell was mounted with a cylinder and hydraulic oil was filled in the annulus between the core and outer cylinder before sealing the cell with 9 bolts (see Fig. 6.1). At the end an LVDT were placed on top of the cell. After all mechanical bits were in place, hydraulic oil was pumped through the confining system to make sure no air was being trapped in the system.

The confining pressure was raised to 0.5 MPa. Cleaning work was performed to ensure less impurity in the test core. Two pore volumes of distilled water were flooded through the core for cleaning purposes. After cleaning, the pore pressure and isotropic stress was pumped up until it reached 0.7 MPa and 1.2 MPa respectively. This was done using a pressure regulating valve connected to a nitrogen-gas (N_2) pressure vessel. The regulator was set to 0.7 MPa, which allows the core to build pore pressure until it reaches 0.7 MPa. Only then will the regulating valve let the brine flow through, and keep the pore pressure from rising further. During this procedure it was important to keep the confining pressure 0.5 MPa above the pore pressure. This was a safety measure to avoid any leakage through the sleeve.

Finally, a pressure regulating valve was placed on the confining outlet while heating elements were turned on to raise the core temperature to 130°C. The pressure regulating valve was adjusted to avoid an extreme pressure due to the expanding oil. After the core had reached desired temperature, the piston was put on top of the core and pressed gradually with a rate of 0.05 ml/min. This was done to make sure that the piston did not hit the core with great power, as this could damage the core and ruin the test. NaCl was introduced as a pre-flooding brine, to minimize the effect of transient creep due to core to core variation, making the comparison of time dependent creep more meaningful.

The following day, the hydrostatic test was initiated. The outlet valve for confining oil was closed, and the confining oil was being pumped at a rate of 0.05 ml/min, raising the confining pressure. This rate was kept constant while the confining pressure reached its target at 11 MPa.

When the confining pressure reached 11 MPa, the creep period was initiated and the confining oil flooding rate was set to 0.5 ml/min with a maximum pressure of 11 MPa.

This was set to avoid the confining pressure to drop. As soon as the pressure drops, the pump would start to pump confining oil until it reached its set pressure. This way, the pressure was kept constant, along with the temperature of 130°C and the flooding rate of 1 PV/day of flooding brine.

During the hydrostatic loading and creep phase, water samples of the flooding brine were collected. Upon completion of creep phase, the flooding brine was switched back to distilled water to clean the plug for 24 hours. This is done to avoid crystallization of the flooding brine inside the core when it is dried after testing. After the final cleaning of the plug, the heating elements were turned off, and the test was complete.

6.5 Brines

A way of measuring the effect of different ions is to flood brine containing different ion compositions. In these experiments the focus has been to validate the importance of magnesium, and also check the effect of pH variance in the flooding brine. The pH is adjusted by adding extremely small amounts of NaOH (0.0126 g). Previous test have confirmed the importance of magnesium and effect of pH (Megawati et al., 2011), but with higher magnesium concentrations than that found in the North Sea reservoirs. By flooding with the same concentration of magnesium of that found in the North Sea seawater, any impact the flooding brine may have on creep deformation must be directly caused by magnesium.

In these experiments, four different compositions of brines were used.

Brine data for all brines are listed in Table 6.3.

Table 6.3: *Brine composition used in these experiments.*

Ions	**Mg_2 + NaOH (w/ NaCl)**	**$MgCl_2$**	**NaCl**	**NaCl + NaOH**
HCO^{3-}				
Cl^-	0.6120	0.4380	0.6570	0.6570
SO_4^{2-}				
Mg^{2+}	0.0445	0.2190		
Ca^{2+}				
Na^+	0.5230		0.6570	0.6570
K^+				
Ionic strength	**0.6570**	**0.6570**	**0.6570**	**0.6570**

7 Results

Three Liège chalk cores were tested; LS7, LS8 and LS9. Although all three cores originated from the same quarry, two cores were drilled from one block, LS8 and LS9, whilst the last core, LS7, was drilled from another.

As a reference, LS8 and LS9 was only flooded with 0.657 M NaCl, with varying pH on LS8 to check if pH variance had any impact without the presence of magnesium. LS7 was first flooded with 0.657 M NaCl, and then switched to pH manipulated, 0.0445 M $MgCl_2$. MS4 was also flooded with NaCl at first, and then switched to 0.219 M $MgCl_2$ with no pH manipulation.

7.1 Liège chalk cores

7.1.1 Mechanical analysis

All cores were flooded with a rate equal to 1 Pore Volume (PV) per day. The cores were analysed during hydrostatic loading and creep phase. For reference, the mechanical properties of the tested cores are presented in Table 7.1

Table 7.1: *Mechanical properties for tested cores*

Chalk core	Length [mm]	Diameter [mm]	Dry weight [g]	Saturated weight [g]	Bulk Volume [ml]	Pore Volume [ml]	Porosity [%]
LS7	71.0	37.0	118.9	150.8	76.3	31.9	41.8
LS8	70.1	37.0	116.2	148.4	75.5	32.2	42.6
LS9	70.1	37.0	115.0	147.5	75.3	32.5	43.1

7.1.1.1 Hydrostatic loading

During hydrostatic loading, all three cores were flooded with 0.657 M NaCl, and the axial stress and strain were measured. Yield point is found during the hydrostatic loading, and can be observed as the stress-strain curve decelerates. The numerical yield point was found by drawing a cross section of the two linear trends found in the elastic and plastic phase in the hydrostatic loading curve (see Fig. 7.1). The yield values for all three Liège cores are presented in Table 7.2.

The bulk modulus, K, was found from the linear slope in the elastic phase in the stress-strain plot and using equation 4.4. As the bulk modulus measures the substance resistance to uniform compression, the strain was considered isotropic. The consequence of using different blocks clearly visualizes in the bulk modulus, K-value. Although all three blocks were collected from the same quarry, they show different porosity, yield strength and bulk modulus. LS7 has lower porosity, yet weaker than LS8 and LS9 – which shows quite similar values with regards to yield strength. LS7 seem to fail more rapidly before yield point, yielding at approximately 8.6 MPa and having reached an axial strain of 0.58%. Both LS8 and LS9 are not yielding before the axial stress has reached 9.14 MPa, with only 0.40% axial strain. Near the end of the hydrostatic test, all three cores seem to deform towards similar strain values, all ending at approximately 1.10% in total axial stress. There does not seem to be a direct relation between yield stress and porosity. All mechanical test results are listed in Table 7.2.

Table 7.2: *Mechanical test results for Liège chalk cores*

Chalk Core	Porosity	Yield Strength	K-value[1]	Total axial strain after hydrostatic loading
LS7	41.8%	8.60 MPa	0.452 GPa	1.10%
LS8	43.1%	9.10 MPa	0.725 GPa	1.07%
LS9	42.6%	9.10 MPa	0.681 GPa	1.06%

[1] K-Value calculated using equation 4.4, whereas the strain has been considered isotropic.

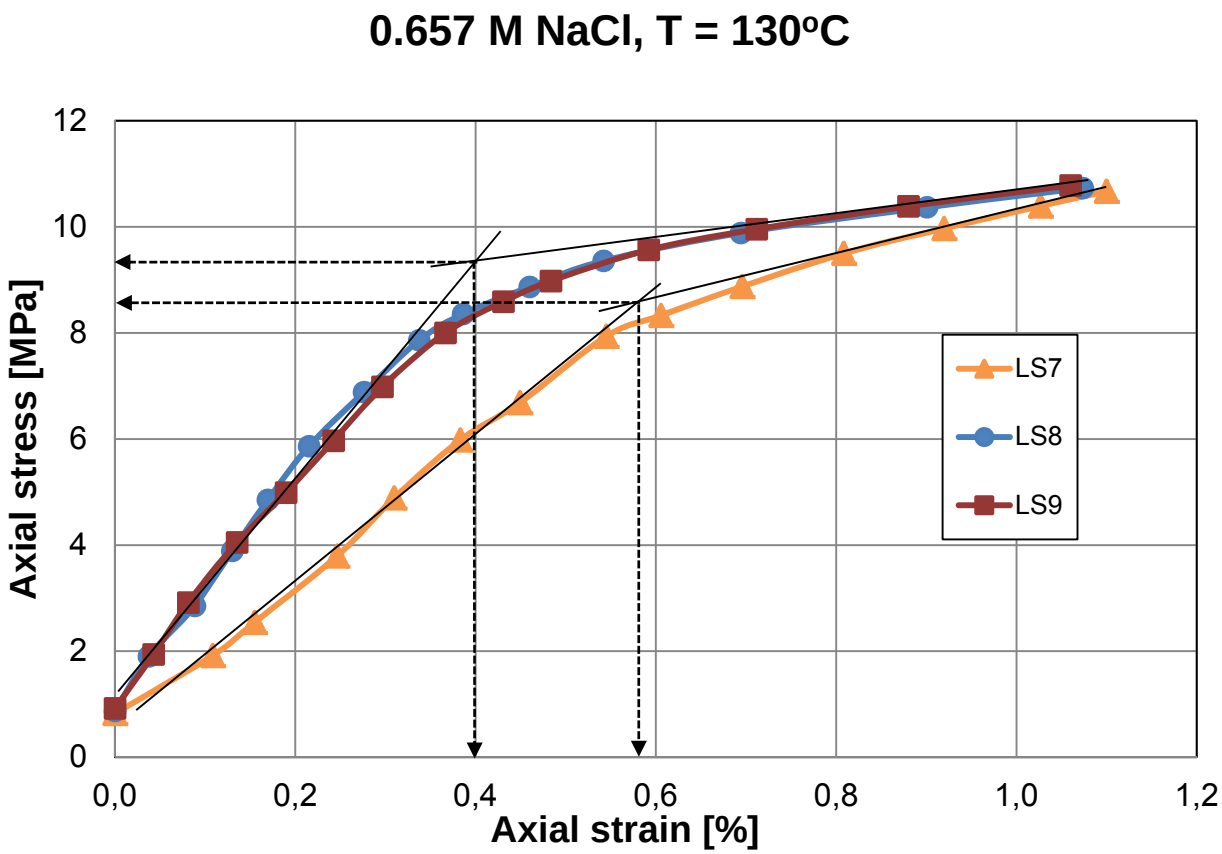

Figure 7.1: *Axial stress [MPa] plotted as a function of Axial Strain [%] for LS7, LS8 and LS9.*

7.1.1.2 Creep phase

Following the end of hydrostatic loading, the creep phase was initiated. During this phase, the chalk cores are left to deform at a constant stress of 11 MPa, and the flooding brines were switched to the desired brines as shown in Table 7.3.

Axial creep strain was plotted versus time, to show how the chalk cores were deformed over time. Time 0 is regarded as the beginning of the creep phase, and the axial creep strain versus creep time for all three Liège chalk cores is presented in Fig. 7.2. As the cores were flooded with a flooding rate of 1 pore volume per day, each day also represents the flooding of one pore volume.

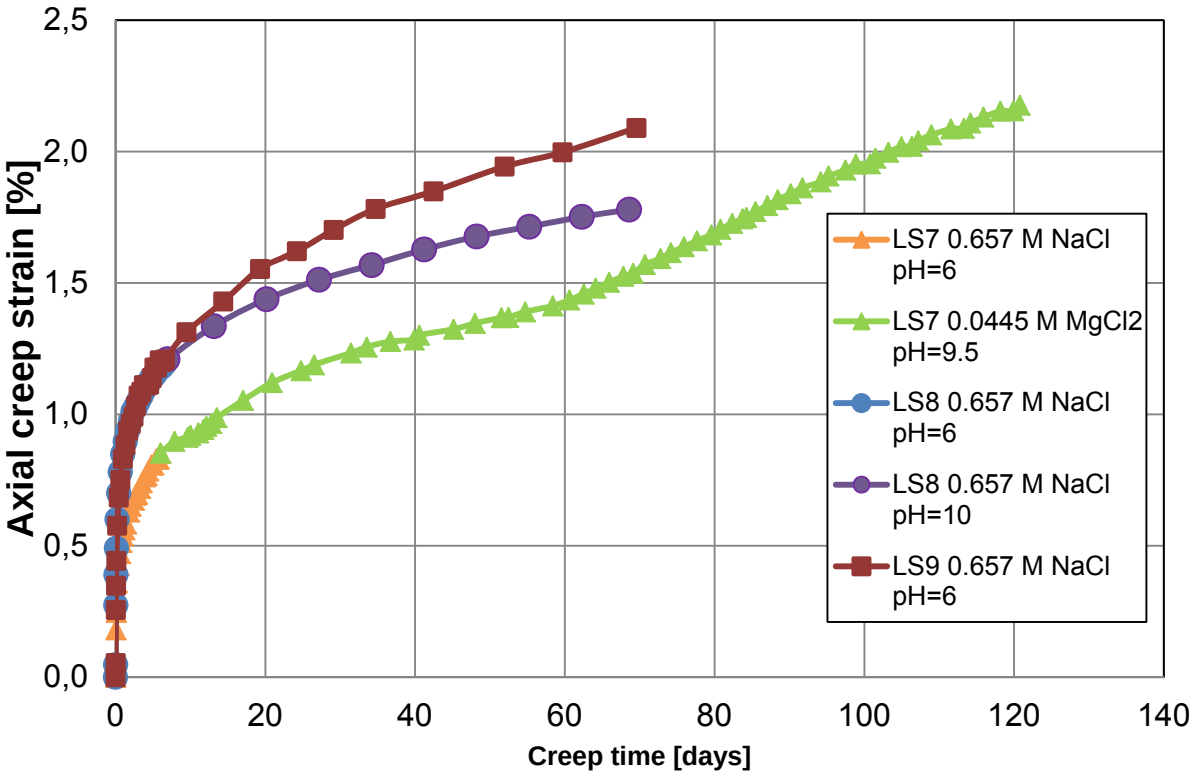

Figure 7.2: *Axial creep strain [%] plotted as a function of creep time [days] for LS7, LS8 and LS9.*

Although LS8 and LS9 were tested on two different triaxial cells, both experienced the same axial creep strain prior to brine switching. This shows that the effect of testing on different triaxial cells is negligible. Both LS8 and LS9 was kept flooding with NaCl, where the pH in LS8 was manipulated after 6.9 days of creep to a pH value of 10. The effect of this pH change is clearly visible on Fig. 7.2, where LS9 kept deforming in the same rate, whilst LS8 seemed to decelerate somewhat. The deformation of LS8 and LS9 was completed after 68.6 and 69.6 days respectively, where LS8 had deformed 1.78% while LS9 had deformed 2.09%.

The impact of using cores from different blocks of outcrop chalk is also visible during the creep phase. Although LS7 was flooded with NaCl the first 6 days, Fig. 7.2 clearly shows a difference in axial creep strain compared to LS8 and LS9. After 6 days of flooding LS7 had deformed 0.85% compared to the 1.20% axial creep strain of LS8 and LS9. At this time, the brine flooding through LS7 was switched to 0.0445M $MgCl_2$ with pH 9.5. Even so, LS7 still kept deforming in the same rate as LS8, which had quite equal pH value. After approximately 60 days of creeping, LS7 experienced an accelerated axial creep strain, ending at a total axial creep strain of 2.18% after 120.8 days of creep.

Table 7.3: *Brine flooding data and resulting axial creep strain*

Chalk core	Flooding fluid	pH	Flooding period [days]		Volume flooded [ml]	Pore volumes	Total axial creep strain [%]	Strain rate, m, after 30 days of creep, [%/decade]	Final Strain rate, m [%/decade][2]
			Start	*Stop*					
LS7	0.657 M NaCl	6	0	6.0	191.4	6.0	0.85	---	---
	0.0445 M $MgCl_2$	9.5	6.0	120.8	3662.1	114.8	2.18	0.69	2.385[3]
LS8	0.657 M NaCl	6	0	6.9	222.2	6.9	1.21	---	---
	0.657 M NaCl	10	6.9	68.6	1986.7	61.7	1.78	0.664	0.664
LS9	0.657 M NaCl	6	0	69.6	2262.0	69.6	2.09	1.021	1.021

A measure to evaluate the axial creep strain is to look at the strain rate, m. This is best shown graphically as presented in Fig. 7.3, where axial creep strain has been plotted as a function of logarithmic creep time. What is of interest here is the last part of each curve; the linear trend. The steeper (more vertical) the trend, the higher strain rate and thus higher rate of deformation.

It is clear from Fig. 7.3 that LS8, with a high pH NaCl, was deforming the chalk at a slower rate than that of lower pH NaCl as indicated from LS9. This is also seen in the strain rates. LS8 had a strain rate of 0.664%, while LS9 had a strain rate of 1.021%. This is a magnitude of 1.54 larger than for that of LS8.

The largest strain rate is seen from $MgCl_2$ flooded core of LS7, which experienced a strain rate of 2.385%. This is significantly larger than what the NaCl flooded cores, even though the pH value was quite similar as that of LS8. With increasing pH, the $MgCl_2$ flooded LS7 experienced a strain rate enlargement due to accelerating creep at the end, whereas the strain rate of NaCl flooded LS8 became smaller.

---

[2] Strain rate, m, was calculated using equation 4.7

[3] Calculated using measurements during steepest part of accelerated creep

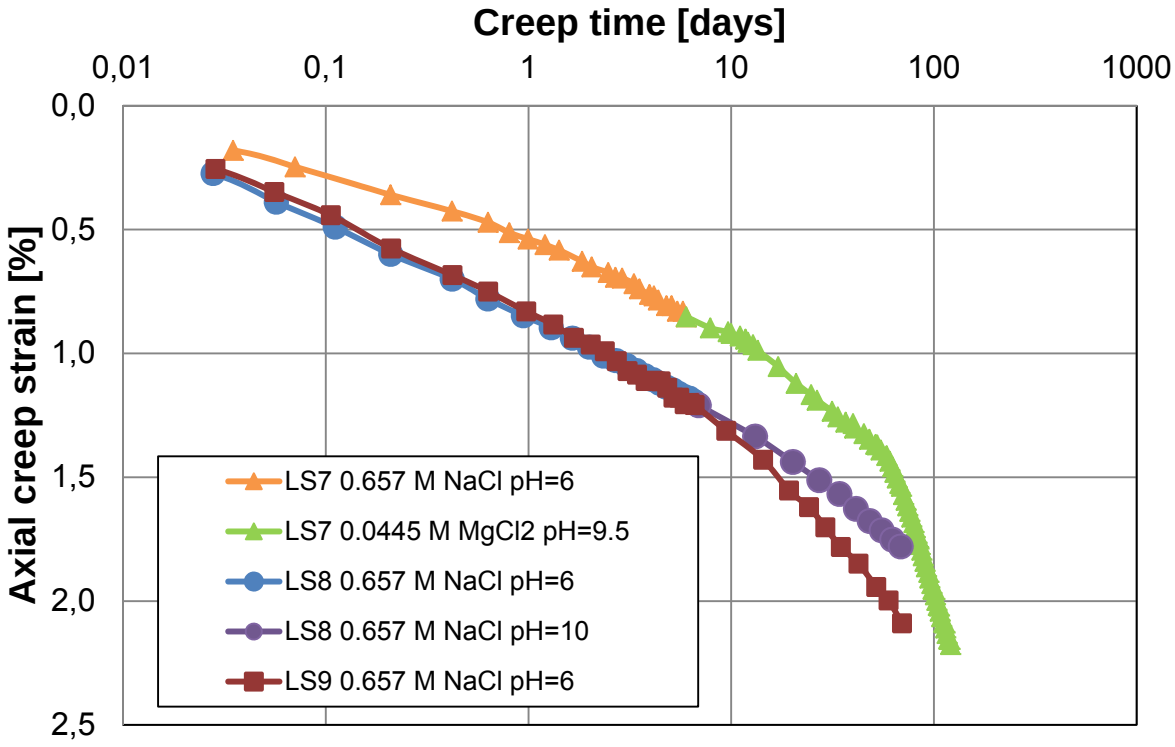

Figure 7.3: *Axial creep strain [%] plotted as a function of logarithmic creep time [days] for LS7, LS8 and LS9.*

7.1.2 Chemical analysis

The ion concentration from the chemical analysis results was plotted as a function of sampling time for the ions present in the effluent brine (see Fig. 7.4 to 7.7)

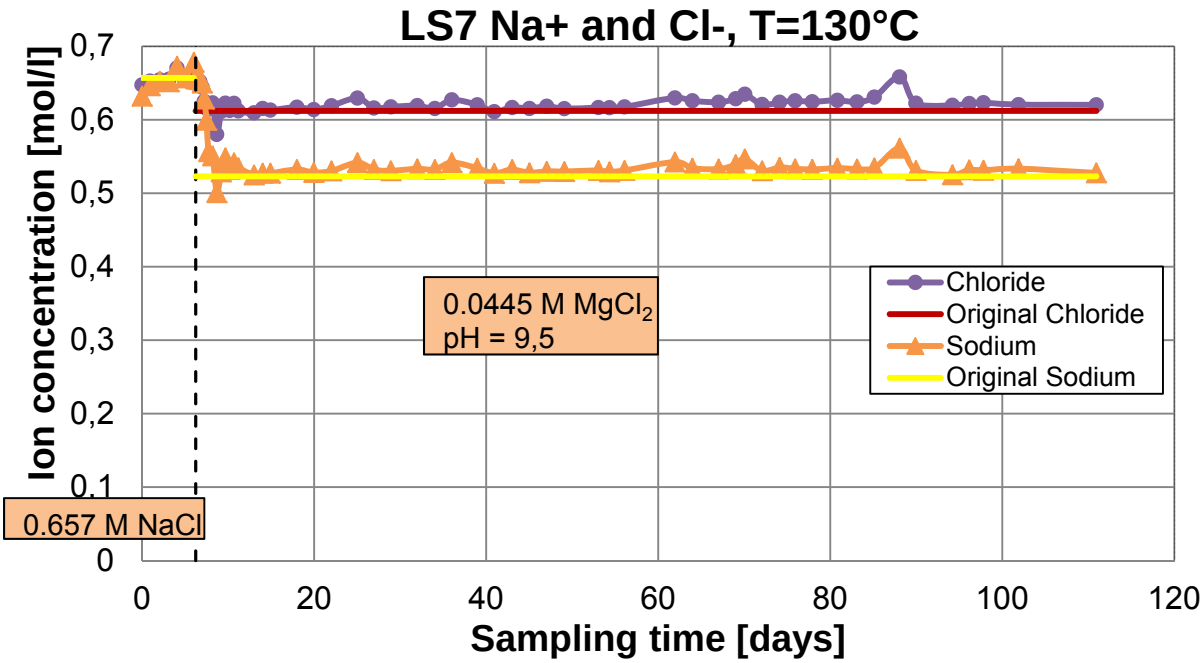

Figure 7.4: *Ion concentration [mol/l] plotted as a function of sampling time [days] for LS8.*

From the effluent water collected from LS7, it was observed that both sodium and chloride concentration fluctuates around their original concentration of 0.657M prior to brine change. After the flooding brine was switched, the sodium concentration was reduced to 0.543M to keep the ionic strength of the 0.0445M $MgCl_2$ brine at equal levels as that of 0.657M NaCl. Even so, the sodium concentration still fluctuates around the original levels of 0,543M.

After $MgCl_2$ was introduced, an immediate calcium production from LS7 was initiated. This is clearly seen from Fig. 7.5 where the magnesium and calcium ion concentrations are plotted as a function of sampling time. The calcium production seems to decrease slowly during the course of time. The magnesium concentration in the effluent does not reach the original magnesium concentration of 0.0445M found in the injecting brine, but seems to increase slowly. When plotting the sum of measured magnesium and calcium concentration in the effluent, they reach the original concentration to that of magnesium in the injecting brine; thus showing that the amount of magnesium loss is equivalent with the calcium production.

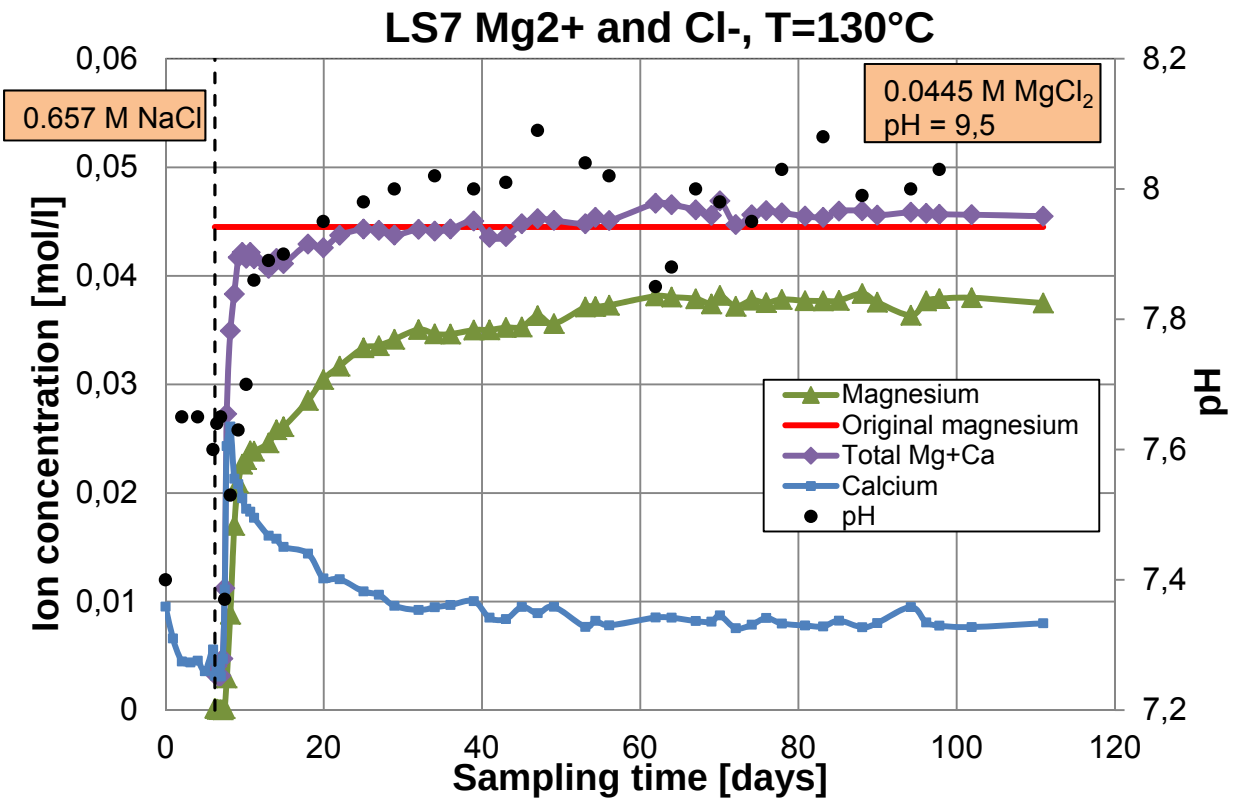

Figure 7.5: *Ion concentration [mol/l] plotted as a function of sampling time [days] for LS7.*

The pH values was measured in all effluent samples, and seemed to fluctuate around a value of pH 8 after the introduction of high pH $MgCl_2$. The measured pH values are presented in Fig. 7.5 as a scatter plot.

For LS8 and LS9, there were little to no change at all to be noted in the effluent compared to the injecting brine. Both sodium and chloride concentrations fluctuated around the original concentration of 0.657M throughout the test. The only discrepancy registered, is a sudden drop of both sodium and chloride concentration in the time interval of approximately 5-12 days, and 37-40 days. This is most likely the result of dilution of the effluent samples.

When considering the calcium ion concentration in the effluent, it is clear that there was no net production of calcium in the effluent to be registered. Ion concentrations found in the effluent from LS8 and LS9 is plotted as a function of sampling time in Fig. 7.6 and 7.7.

The pH values seem to fluctuate around 7.6 – 7.8 for both LS8 and LS9, even though LS9 was injected with a higher pH brine. For LS7, the pH also fluctuates around 7.6 prior to injection of magnesium containing brine, whereas the pH values are a bit higher, fluctuating at around pH 8.

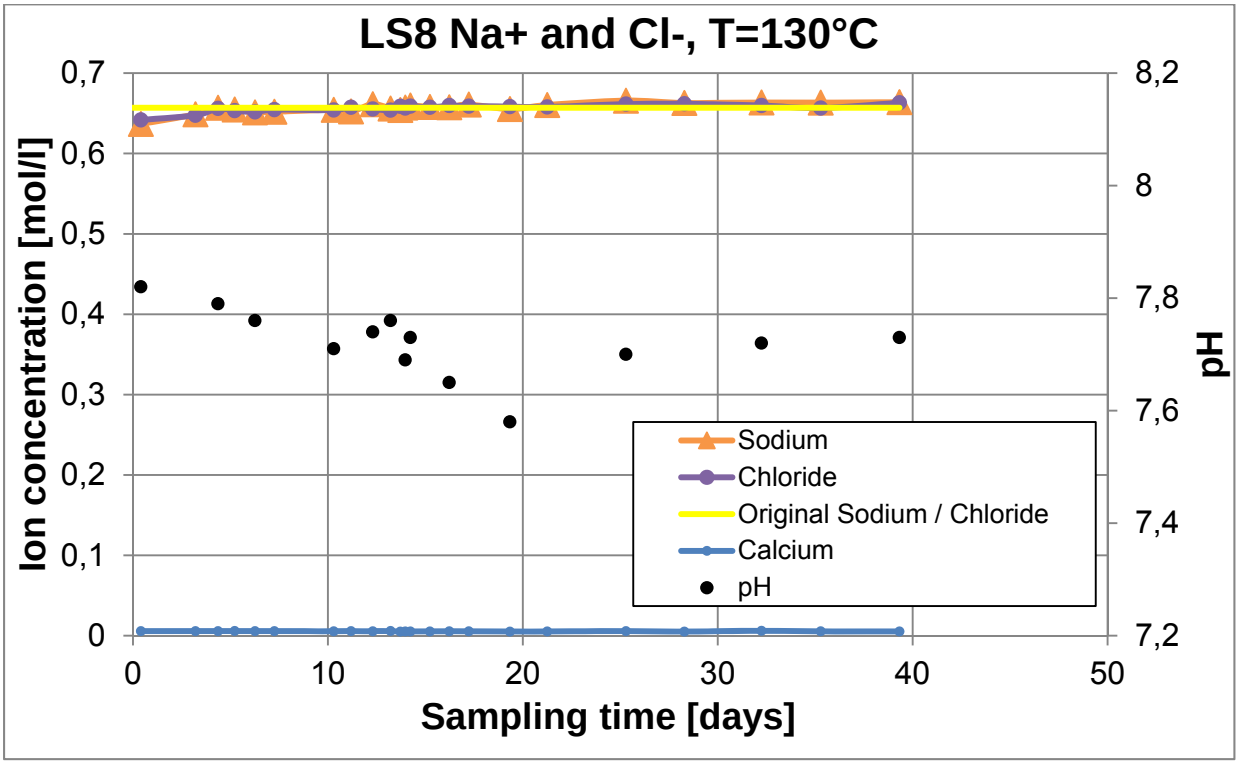

Figure 7.6: *Ion concentration [mol/l] plotted as a function of sampling time [days] for LS8.*

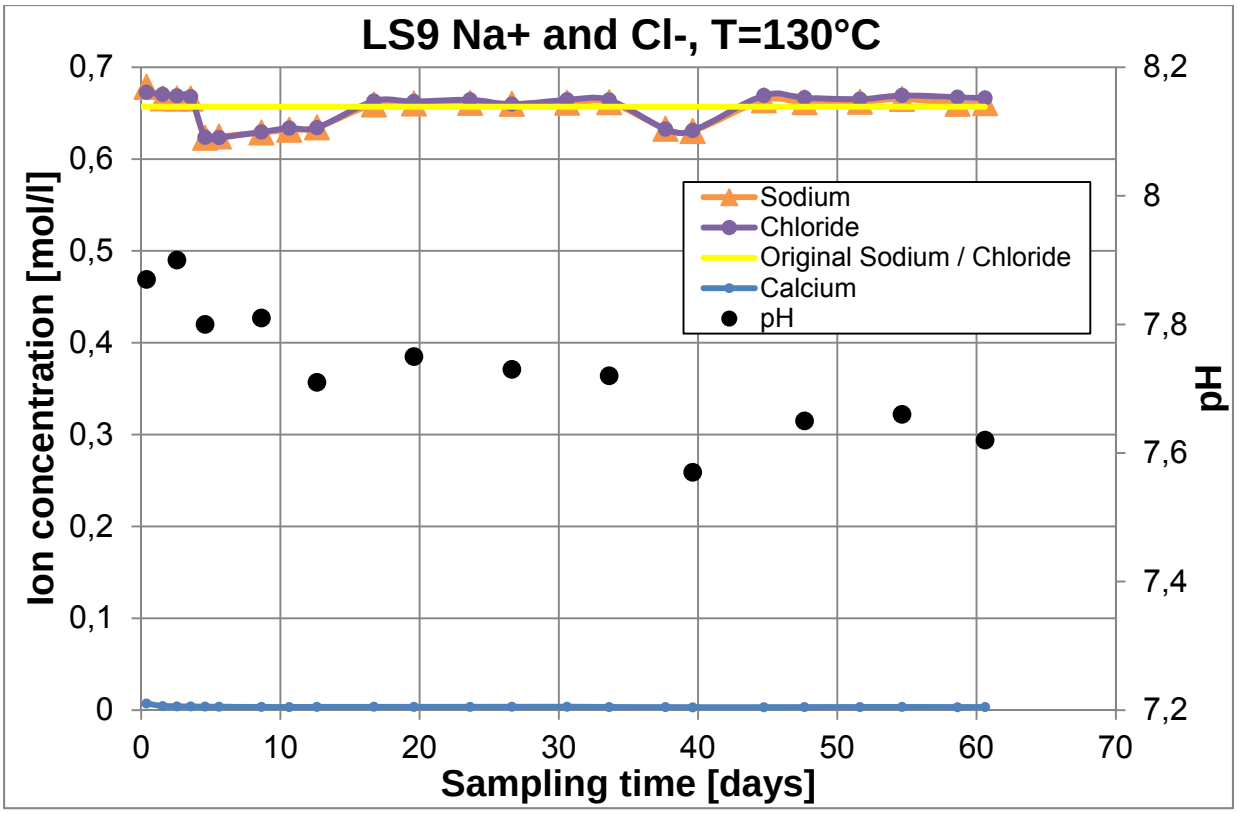

Figure 7.7: *Ion concentration [mol/l] plotted as a function of sampling time [days] for LS9.*

7.2 Mons chalk cores

7.2.1 Mechanical analysis

The chalk core was flooded with a rate equal to 1 Pore Volume (PV) per day. The core was analysed during hydrostatic loading and creep phase. For reference, the mechanical properties of the tested core are presented in Table 7.4.

Table 7.4: *Mechanical properties of MS4*

Chalk core	Length [mm]	Diameter [mm]	Dry weight [g]	Saturated weight [g]	Bulk Volume [ml]	Pore Volume [ml]	Porosity [%]
MS4	70.5	37.0	114.5	147.3	75.8	32.8	43.3

7.2.1.1 Hydrostatic loading

During hydrostatic loading, the core was flooded with 0.657M NaCl, and the axial stress and strain was measured. Both yield point and bulk modulus, K, was found as described in chapter 7.1.1.1. MS4 experienced yield at around 9.9 MPa and experienced a total axial strain of 1.05% during hydrostatic loading. All mechanical test

results presented in Table 7.5 and axial stress is plotted as a function of axial strain during hydrostatic loading in Fig. 7.8

Table 7.5: *Mechanical test results for MS4*

Chalk Core	Porosity	Yield Strength	K-value[4]	Total axial strain after hydrostatic loading
MS4	43.4	9.90 MPa	0.773 GPa	1.05%

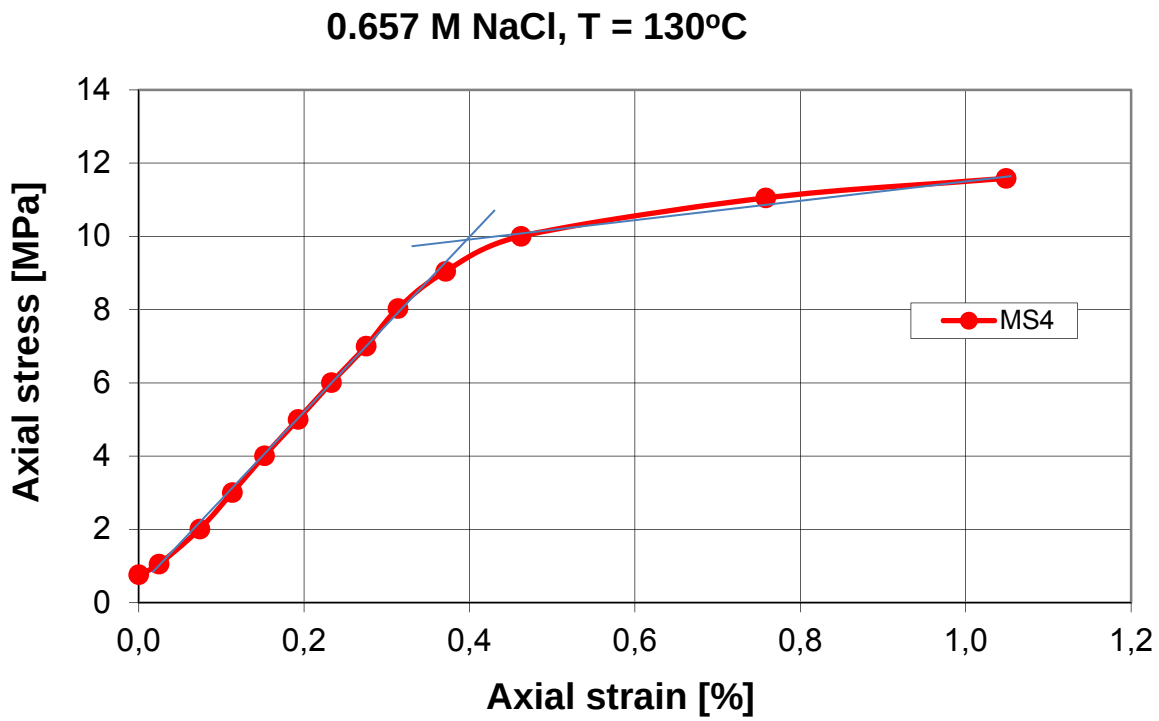

Figure 7.8: *Axial stress [MPa] plotted as a function of Axial Strain [%] for MS4.*

7.2.1.2 Creep phase

Following the end of hydrostatic loading, the creep phase was initiated. During this phase, the chalk core was left to deform at a constant stress of 12 MPa, and the flooding brine was switched to the desired brine as shown in Table 7.6. The reason why MS4 was left to deform at a constant stress of 12 MPa as opposed to the Liège chalk cores, which were left to deform at 11 MPa, is that Mons chalk is known to be

[4] K-Value calculated using equation 4.4, whereas the strain has been considered isotropic.

somewhat stronger with regards to yield. This is also seen in this case, where the Liège chalk cores experienced yield at approximately 1MPa less than that of MS4.

Axial creep strain was plotted versus time, to show how the chalk cores were deformed over time. Time 0 is regarded as the beginning of the creep phase, and the axial creep strain versus creep time for MS4 is presented in Fig. 7.9.

After the flooding brine had been switched to $MgCl_2$, it seemed as though the deformation process abruptly ended. The flooding brine was switched after 6 days of creeping, at that stage at an axial creep strain of 1.22%. After further 26 days of creeping, total axial creep strain had increased only to 1.41%, but it was at this time that **accelerating creep** was observed. The characteristics of accelerating creep seemed to be subject to a time delay, not occurring until the core had been flooded with Mg2+ ions for 26 days. This evidently suggests that the accelerated creep phase cannot be a result of a short delayed response to the new flooding brine introduced. After 121 days, total axial creep strain ended at 5.62%. All creep data is listed in Table 7.6.

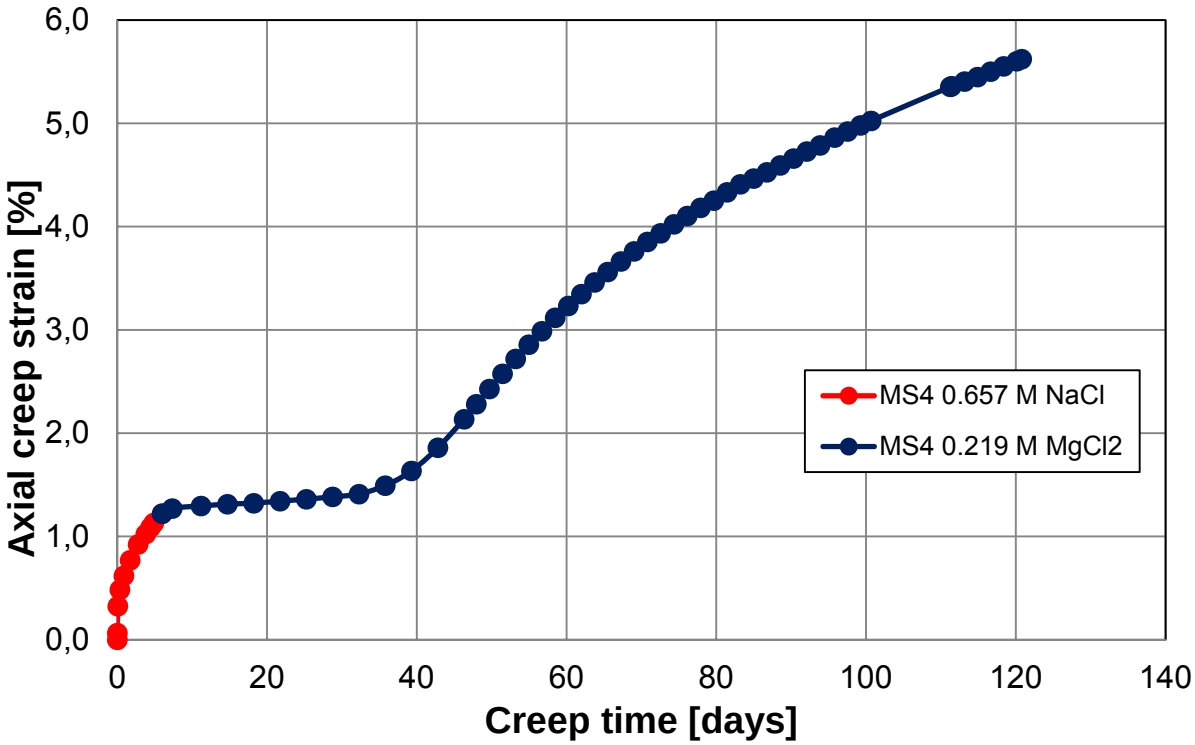

Figure 7.9: *Axial creep strain [%] plotted as a function of creep time [days] for MS4.*

Table 7.6: *Brine flooding data and resulting axial creep strain*

Chalk core	Flooding fluid	pH	Flooding period [days]		Volume flooded [ml]	Pore volumes	Total axial creep strain [%]	Strain rate, m, after 30 days of creep, [%/decade]	Final Strain rate, m [%/decade][5]
			Start	*Stop*					
MS4	0.657M NaCl	6	0	6.0	196.8	6.0	1.22	---------	---------
	0.219M $MgCl_2$	9.5	6.0	120.8	3662.1	114.8	5.62	0.24	9.204[6]

The axial creep strain was also plotted as a function of logarithmic time to calculate the strain rate, see Fig. 7.10. The strain rate, m, prior to the accelerated creep phase (after 30 days of creep) was calculated to be 0.24%/decade, whilst during the accelerated creep the strain rate was calculated to be 9.204%/decade; a magnitude of more than 38 times larger. The measurements from these calculations were taken from the steepest part of the accelerating strain, as it is this part of the creep period which is of interest. After the core has deformed for a substantial period of time, the axial creep strain will always diminish with time as the core gets more and more compacted.

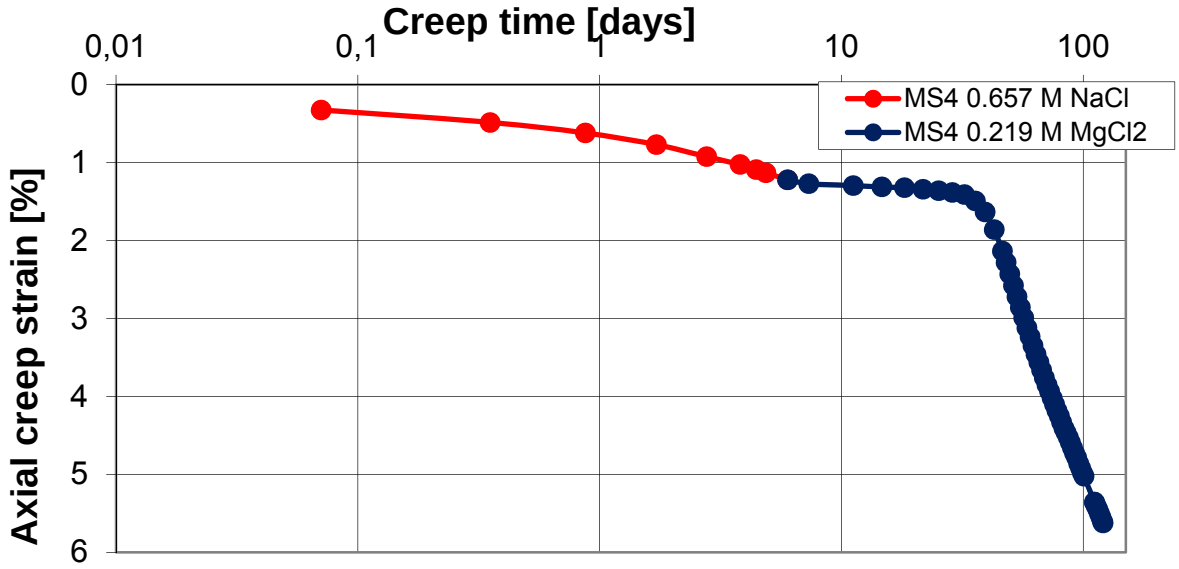

Figure 7.10: *Axial creep strain [%] plotted as a function of logarithmic creep time [days] for MS4.*

[5] Strain rate, m, was calculated using equation 4.7

[6] Calculated using measurements during the steepest part of the accelerated creep

7.2.2 Chemical analysis

The ion concentration from the chemical analysis results was plotted as a function of sampling time for the ions present in the effluent brine (see Fig. 7.11 and 7.12)

For MS4, both sodium and chloride concentration fluctuate around their original concentration of 0.657M prior to brine any change. When changing the brine to 0.219M $MgCl_2$, sodium concentration drops to zero (which is expected as there is no sodium present in the injection $MgCl_2$ brine). The chloride concentration reaches and fluctuates around a concentration of 0.438M, which equals to that found in the original $MgCl_2$ brine (see Fig. 7.11)

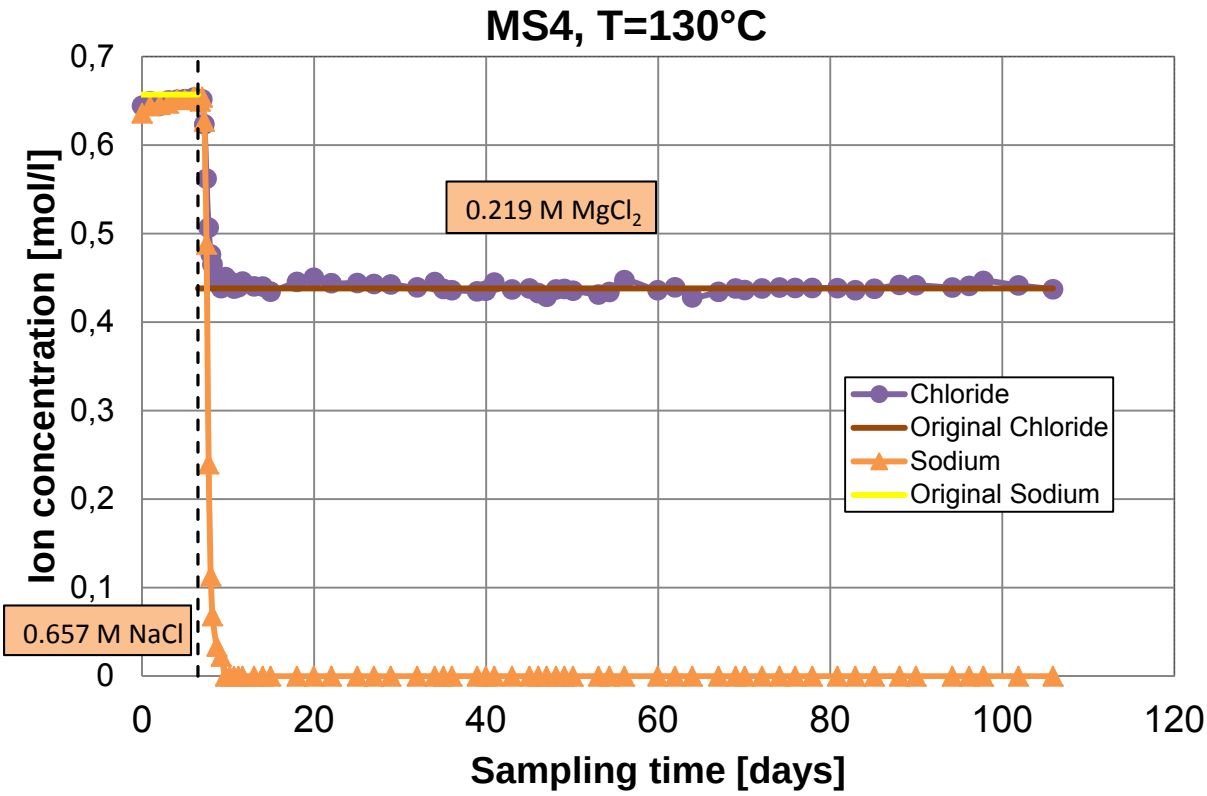

Figure 7.11: *Ion concentration [mol/l] plotted as a function of sampling time [days] for MS4.*

Prior to the substitution of brine, there is little or no calcium being produced from the chalk core. Immediately after the new brine is introduced, calcium production is at its largest (0.033 mol/l), and gradually declining until approximately 27 days of sampling. It is at this time, at start of accelerating creep, that the calcium production gradually rises and continues to do so until the end of the test. The opposite applies for magnesium, where immediately after brine change a magnesium concentration is noted in the effluent. This concentration does not reach the original concentration of

0.219M, which indicates that some magnesium is left within the chalk core. A gradual increase of magnesium is seen until approximately 27 days of sampling, where it starts to gradually decrease again. If the magnesium concentration in the effluent is added with the calcium concentration being produced, the sum fluctuates around that of the original magnesium concentration (see Fig. 7.12).

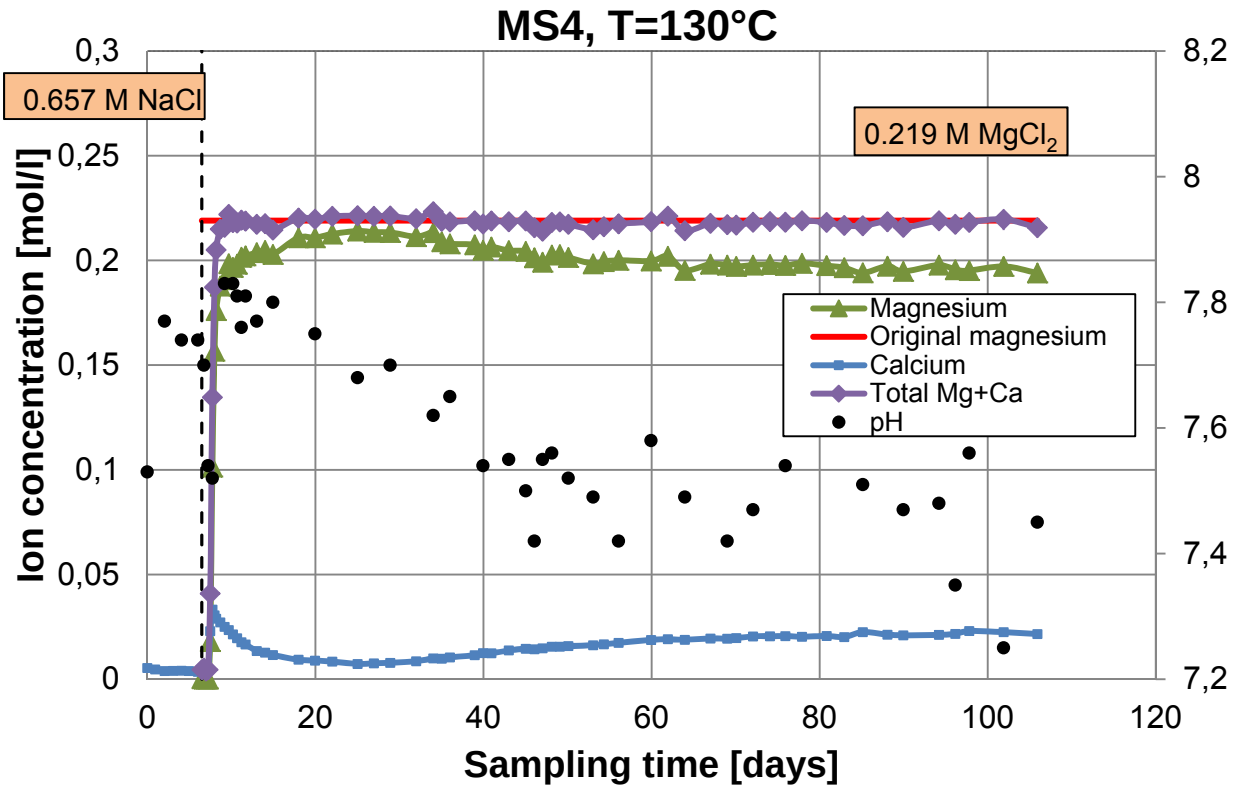

Figure 7.12: *Ion concentration [mol/l] plotted as a function of sampling time [days] for MS4.*

As seen from Fig. 7.12, the pH values in the effluent seem to diminish slightly from start of injection of $MgCl_2$ to start of accelerated creep phase. At this stage, the pH values seem to stabilize at around a pH level of 7.5.

8 Discussion

The results from the mechanical tests clearly show that the compositions of the flooding brine have a major impact on the mechanical behavior of the chalk. Although the difference in pH did not show tremendous difference in axial creep compaction behavior, it did indicate that pH of the flooding brine may also play a certain role when considering the rock-fluid interaction of flooding brines on chalk.

It could also be seen that the purity of the outcrop chalk may also play an important role when considering the impact of the flooding brines. The mechanical test results for all tested cores are presented in Table 7.7.

Table 8.1: *Mechanical test results for all cores tested.*

Chalk Core	Outcrop	Flooding brine	pH	Porosity	Yield Strength	K-value [7]	Total axial creep strain	Strain rate, m, after 30 days of creep	Final Strain rate [8]
LS7	Liège	0.0445M $MgCl_2$	9.5	41.8%	8.60 MPa	0.452 GPa	2.18%	0.69 %/decade	2.385 %/decade
LS8	Liège	0.657M NaCl	10	42.6%	9.10 MPa	0.725 GPa	1.78%	0.664 %/decade	0.664 %/decade
LS9	Liège	0.657M NaCl	6	43.1%	9.10 MPa	0.681 GPa	2.09%	1.021 %/decade	1.021 %/decade
MS4	Mons	0.219M $MgCl_2$	6	43.3%	9.90 MPa	0.773 GPa	5.62%	0.24 %/decade	9.204 %/decade

[7] K-Value calculated using equation 4.4, whereas the strain has been considered isotropic.

[8] Strain rate, m, was calculated using equation 4.7 and measures from the steepest part of the curve has been used

8.1 Differences in mechanical strength during hydrostatic loading (1 PV/day 0.657 M NaCl)

As seen from Table 8.1, there is quite a difference with regards to mechanical strength when considering the bulk modulus, K, and yield strength of LS7 and LS8 / LS9. All these cores are from the same outcrop; however they were not drilled from the same block as there were no more cores available from the first block used. As the outcrop blocks were not marked with indication of bedding direction, this might result in the cores being drilled in different directions, i.e. one in horizontal direction whilst the other in vertical direction (see Fig. 8.1). In Korsnes et al. (2008), the effect of anisotropy on mechanical properties of outcrop chalk was studied. This was done by drilling samples horizontally and vertically from the same chalk block. Their studies showed that the difference in yield strength for Liège chalk was a factor of 1.44 larger for chalk cores drilled in vertical direction compared to horizontal direction. Bedding direction was not known in this paper either. It was also reported that the bulk modulus for Liège chalk cores drilled in vertical direction was a magnitude of 1.50 larger than that of horizontal direction, and that it could be seen that the samples with the highest yield stress obtained the highest bulk modulus.

As seen in Table 8.1, the bulk modulus for LS8 and LS9 is quite similar, which is to be expected as they both originate from the same block and was drilled in the same direction. However, the bulk modulus for LS7 is a magnitude of 1.60 and 1.51 smaller than that of LS8 and LS9 respectively. When considering the yield values for the three Liège cores, these also differ from one another. While the yield strength of LS8 and LS9 are both 9.10 MPa, the yield value for LS7 is 8.6 MPa; a factor of 0.94 smaller than that of LS8 and LS9. What is also interesting to note, is how much the chalk core had deformed when reaching yield. LS8 and LS9 had only experienced an axial strain of 0.40%, while LS7 had experienced an axial strain of 0.58%; a magnitude of 1.45 larger than that of LS8 and LS9.

These results coincide exceptionally well with the results presented by Korsnes et al. (2008), with the exception of the yield stress, which does not differ in the same magnitude. However, considering that the bulk modulus differed in the same magnitude as presented by Korsnes et al. (2008), and that the fact that it could also be observed in these tests that the chalk core with the highest yield stress obtained the

highest bulk modulus, it may be established that these differences in mechanical strength may be directly caused by the difference in drilling direction; indicating that LS8 and LS9 was drilled in vertical direction, while LS7 was drilled in horizontal direction. As mentioned, the bedding direction of the outcrop block was not known, and hence cannot be established based on the comparison with the results from Korsnes et al. (2008). However, it is reasonable to assume that chalk cores drilled vertically with respect to bedding direction should be mechanically stronger than horizontally drilled cores, considering that due to the larger overburden stresses experienced in vertical bedding direction the chalk core should be more solid and hence have a higher yield stress.

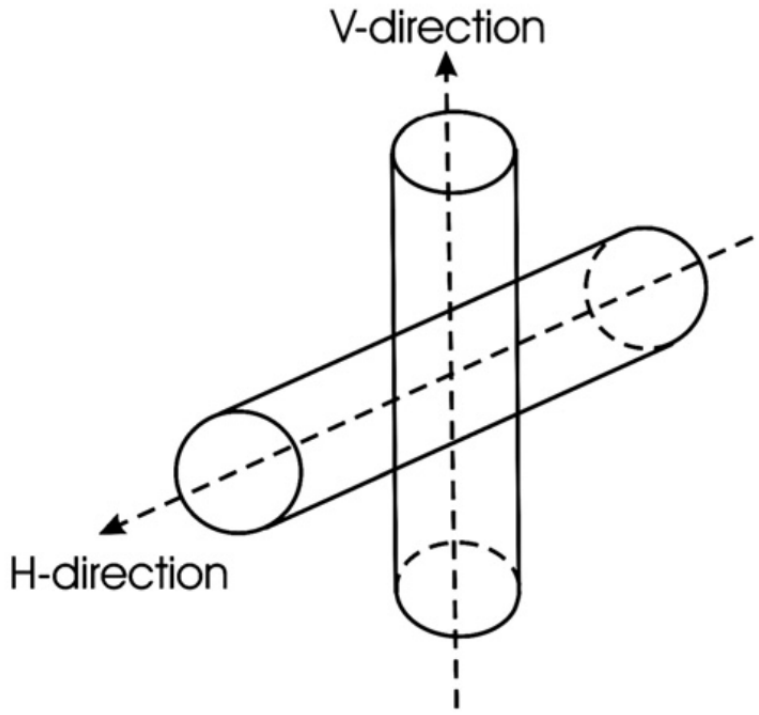

Figure 8.1: *Schematic illustration of samples drilled perpendicular to each other (Korsnes et al., 2008).*

When considering the mechanical strength during hydrostatic loading of Mons chalk, it is clear from Fig. 8.2 and Table 8.1 that there is quite a difference in yield stress compared to Liège chalk. The Liège chalk has yield strengths in the range of 8.60MPa to 9.10MPa, while the Mons chalk core experienced yield at 9.9MPa; 9-15% larger than that of Liège. However, the bulk modulus indicates that these outcrop chalks does not behave in the same manner. While for Liège, there was a clear correlation between the magnitude of the bulk modulus and yield strength, but the same

correlation is not seen from the hydrostatic loading results from Mons chalk. Although the yield stress is larger, the bulk modulus of MS4 is quite equal to those of LS8 and LS9, as seen from Table 8.1. This may indicate that Mons chalk is mechanically stronger than that of Liège with similar porosity.

The two quarries are located quite close to each other (approximately 130km), both from the same age and are characterized by a similar geodynamical context (Darquennes et al., 2007). This difference in mechanical strength may be caused by the difference of carbonate content between the two outcrops. Previous studies (Madland et al., 2011) have shown that seawater induced compaction increases with increasing non-carbonate content. Considering that the Mons chalk is cleaner with respect to carbonate content, this may in fact cause the chalk to be mechanically stronger.

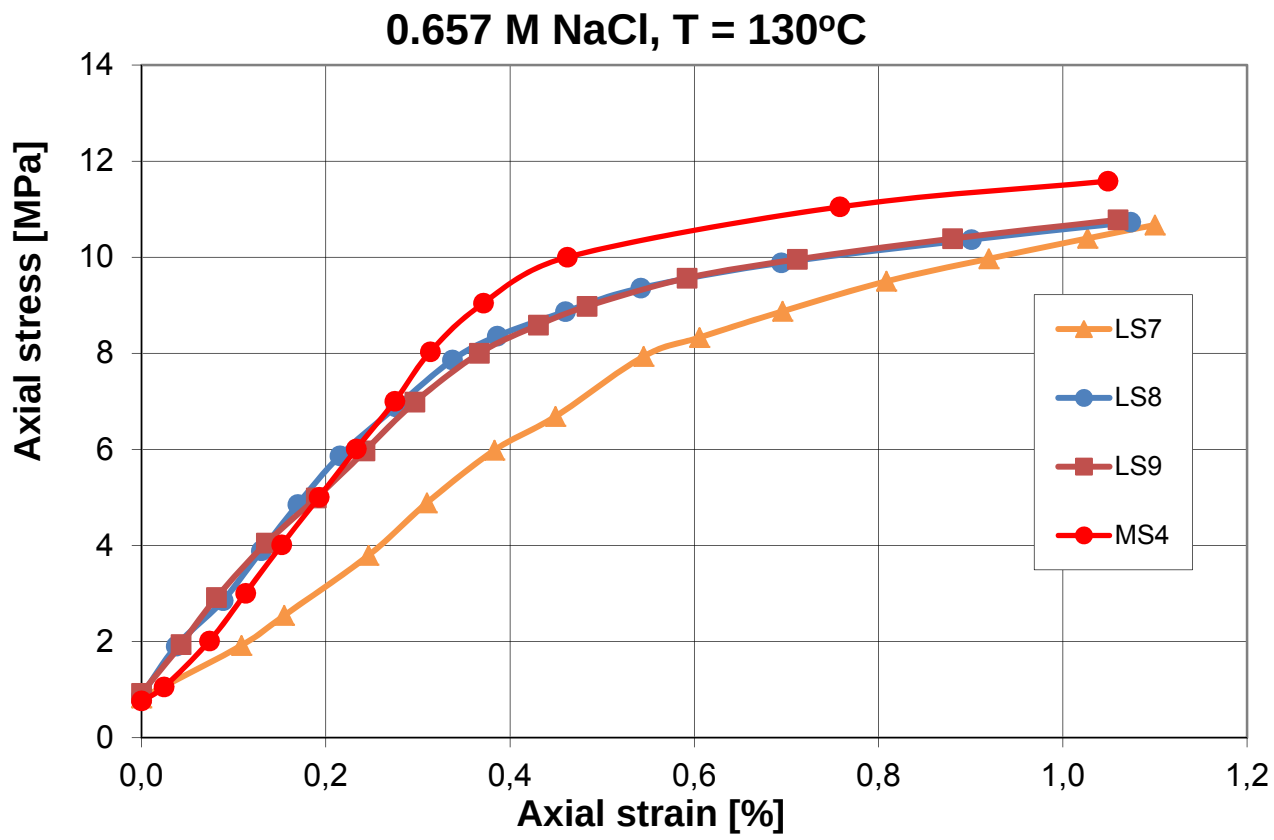

Figure 8.2: *Axial stress [MPa] plotted as a function of Axial Strain [%] for all tested cores.*

8.2 Creep phase analyses

When comparing the axial creep strain of all tested cores (see Fig. 8.3), it is clear that magnesium plays an important role when considering the water weakening effect of chalk caused by the flooding fluid. The importance of the presence of magnesium during different part of the creep phase and the effect of pH is further discussed in the following subchapters.

8.2.1 The effect of chalk purity

Immediately after the flooding brine for MS4 had been switched to 0.219 M $MgCl_2$, the deformation process seems to almost flatten, with a strain rate of only 0.24%/decade. This strain rate is kept constant for approximately 20 days, until an accelerated creep phase is initiated.

In Madland et al. 2011, similar studies were performed, but with Stevns Klint and Liège chalk cores flooded with non pH adjusted 0.219 M $MgCl_2$. The observation of decelerating creep after switching to magnesium containing brine was also observed from the Stevns Klint chalk cores, however not from the Liège chalk cores, even though both outcrop chalks were flooded under the same conditions and with the same flooding brine. The Liège core obtained a strain rate of 1.78%/decade, whilst the Stevns Klint core obtained a strain rate of 0.11%/decade. Comparing these results with the results from MS4, this may suggest that the abrupt decline (and almost ending) of the creep compaction after introducing the $MgCl_2$ brine, may be associated with the purity of the outcrop chalks; as both Mons and Stevns Klint are highly pure outcrop chalks (calcite content of 99.8% for Stevns Klint (Hjuler and Fabricius 2009)). This immediate decelerating effect on deformation that magnesium has on pure chalk was also presented by Zhang et al. (2002), but under quite different conditions (super pure calcite powder under room temperature with an applied stress of 4 MPa in one direction only). They could not observe any accelerating creep compaction, and even concluded Mg^{2+} ions to be a well-known inhibitor of calcite precipitation. However, this only illuminates the importance of temperature on the proposed dissolution-precipitation process, as magnesium evidently has a profound effect on the creep compaction as observed by the following accelerated creep phase to that of MS4 (see Fig. 8.3).

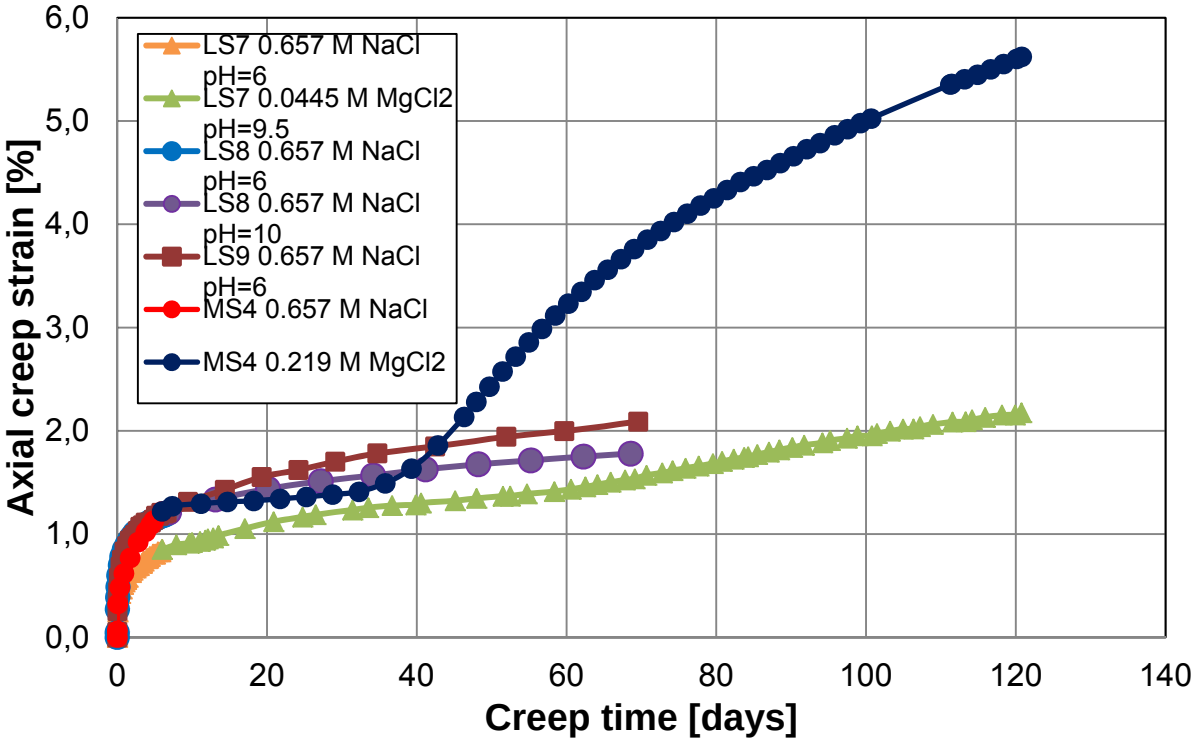

Figure 8.3: *Axial creep strain [%] plotted as a function of creep time [days] for all tested cores.*

8.2.2 The effect of varying concentration of magnesium with regards to accelerated creep

As seen from Fig. 8.3, the only chalk cores which experience an accelerated creep compaction, are in fact those flooded with magnesium containing brines. This is best seen from MS4, which experienced axial creep strain in the magnitude of more than 2.5 larger than that of cores flooded with non-magnesium containing brines. The importance of magnesium as the key ion, when considering the dissolution-precipitation process, has also previously been thoroughly examined (Megawati et al., 2011; Madland et al., 2011). The importance of magnesium is also well noticed when comparing the ion concentration found in the effluent brine to the axial creep strain of MS4 (see Fig. 8.4). At the beginning of creep phase, magnesium concentration is steadily increasing in combination with a steady decline in calcium concentration. This implies that magnesium is reaching equilibrium with calcium in the calcite. As the accelerated creep phase is initiated after approximately 29 days (marked on Fig. 8.4 as the dotted black line), an increased calcium production in addition to a decreased magnesium concentration in the effluent can be observed. This further suggests that

secondary magnesium bearing minerals are being precipitated, as calcite is being dissolved, resulting in enhanced creep compaction as observed by the accelerating creep phase. The combination of accelerated creep and an increased calcium production / magnesium retention was also observed by Megawati et al. (2011), but with Liège cores flooded by pH adjusted 0.219 M $MgCl_2$ (see Fig. 8.6), and by Madland et al. (2011), where Stevns Klint cores were flooded by non pH adjusted 0.219 M $MgCl_2$.

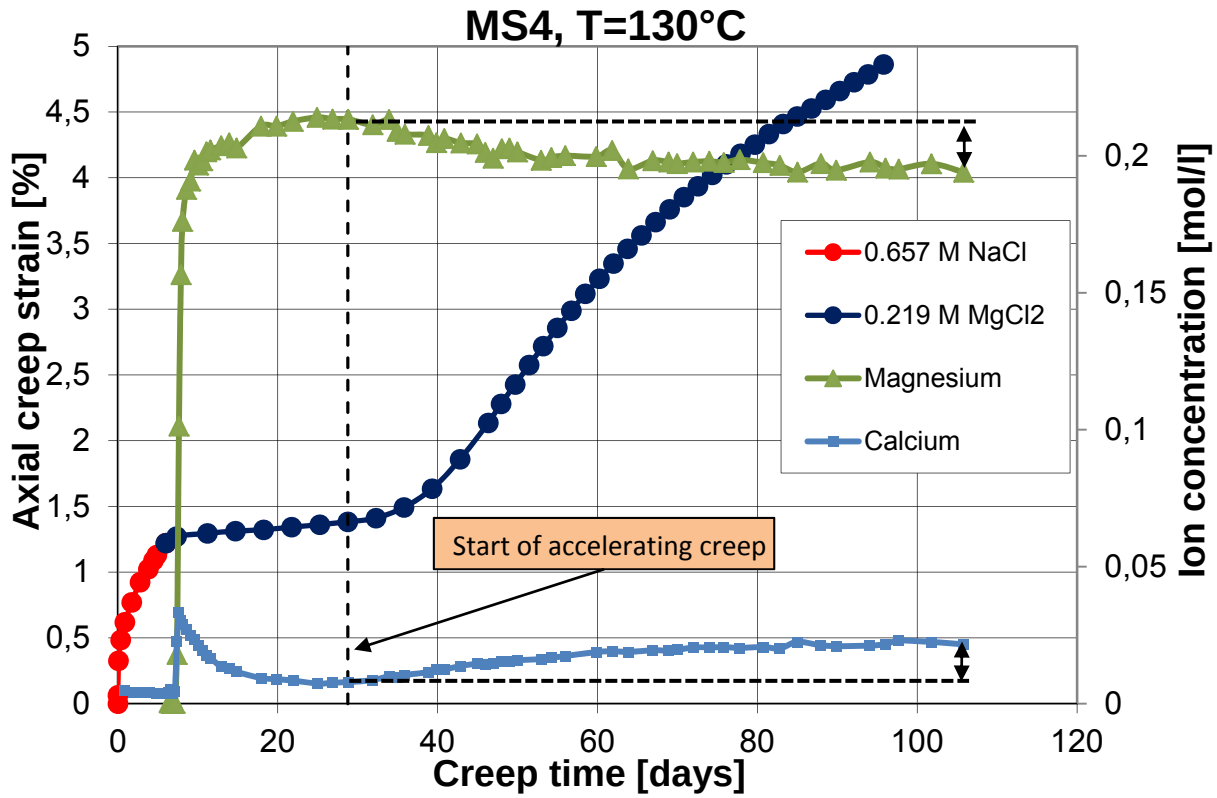

Figure 8.4: *Axial creep strain [%] and ion concentration of the effluent brine [mol/l] plotted as a function of creep time [days] for MS4.*

When considering the Liège chalk cores tested in this study, it is also notable that the only chalk core that experiences accelerated creep is the core flooded with a magnesium containing brine (LS7). The strain rate of LS7 is considerably lower than that of MS4 chalk during the accelerated creep phases (see Table 8.1); a magnitude of 3.86. The magnesium concentration for the brine flooded through LS7 was only 0.0445 M compared to that of the 0.219 M concentration which was flooded through MS4; a magnitude of 4.92 larger for MS4 than that of LS7. This clearly indicates that there may be some correlation between the amount of magnesium being flooded through the core, and the axial creep strain that the core experiences. This process is also

seen in Fig 8.5 as it was seen with MS4; a steady rise in magnesium concentration in combination with a decline in calcium concentration can be observed in the beginning of the creep phase. However, at the initiation of accelerated creep phase both calcium and magnesium concentrations seem to stabilize, contrasting to that of MS4. One logic explanation to this dissimilarity might be that MS4 and LS7 originate from different outcrops. However, the results shown by Megawati et al. (2011), where a Liège chalk core (LEM8) was flooded with pH adjusted 0.219 M $MgCl_2$ (pH=9.3), shows that at the same magnesium concentrations, it behaves similar to that of MS4 during accelerating creep; an increase in calcium concentration and decrease in magnesium concentration is clearly observed as shown in Fig. 8.6. This further demonstrates that, considering that the only difference between LS7 and LEM8 was in fact the magnesium concentration, the accelerated creep phase experienced by LS7 may be caused by other processes than that of LEM8 and MS4.

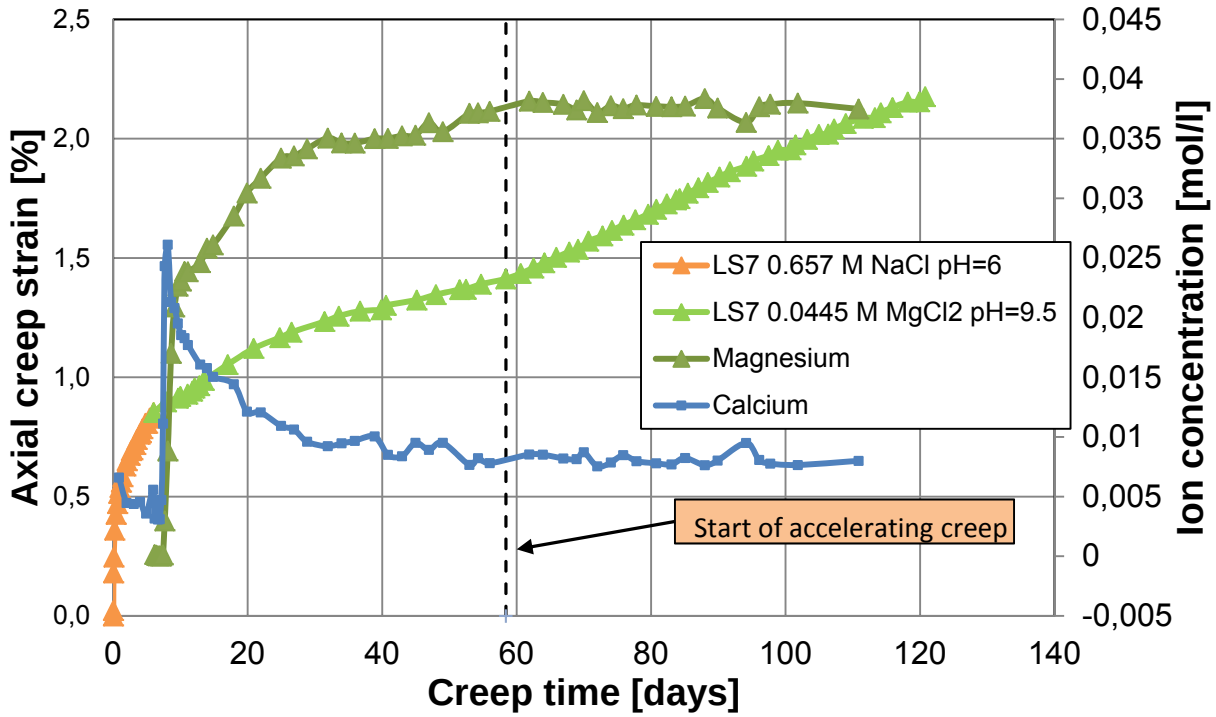

Figure 8.5: *Axial creep strain [%] and ion concentration of the effluent brine [mol/l] plotted as a function of creep time [days] for LS7.*

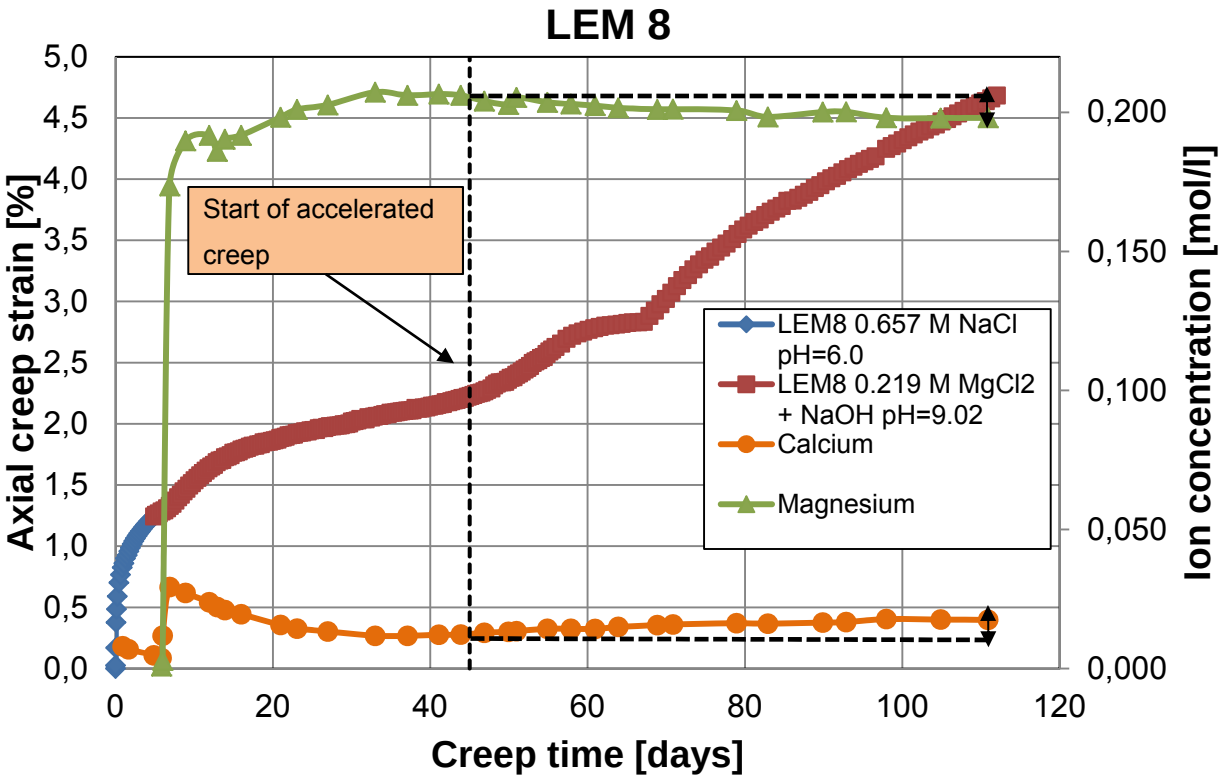

Figure 8.6: *Axial creep strain [%] and ion concentration of the effluent brine [mol/l] plotted as a function of creep time [days] for LEM8 (Megawati et al, 2011).*

8.2.3 The effect of pH

It is well established that the rate of pure dissolution of calcite increases with decreasing pH. This is also observed in Fig. 8.3, where LS9 is deforming at a higher rate than that of LS8, where both cores are flooded with 0.657M NaCl but with different pH values; LS8 with a pH of 10 and LS9 with a pH of 6. However, this does not seem to be the case when magnesium is present in the flooding brine. Even at very low magnesium concentrations (0.0445 M) equalling that found in seawater, an accelerated creep compaction is observed. The cause of this accelerated creep compaction might involve the non-carbonate minerals present in the chalk core, which commonly fill the intergranular voids (Fabricius et al., 2007). Megawati et al. (2011) suggested that if these non-carbonate minerals do play a role as contact cement in which keeps the calcite grains connected, any chemical modification in which involves cement will consequently have a great effect on the mechanical characteristics. It was also suggested that any chemical modifications that does involve the non-carbonate minerals could be a predecessor to slide off the support carried by the contact points. With this as a basis, there is a possibility that when flooding with high pH $MgCl_2$, the

cause of the accelerated creep compaction might be the dissolution of non-carbonate minerals involving silica and clay minerals. This is further supported by the fact that at higher pH values, the solubility of silica in water increases rapidly due to ionization and polymerization (White et al., 1998). It was also reported by Moller et al, (2006) that dissolution of aluminium silicate minerals through the hydrolysis and detachment of Al and Si from the mineral framework has shown to be pH dependent, with increasing solubility the higher the pH (see Fig. 8.7).

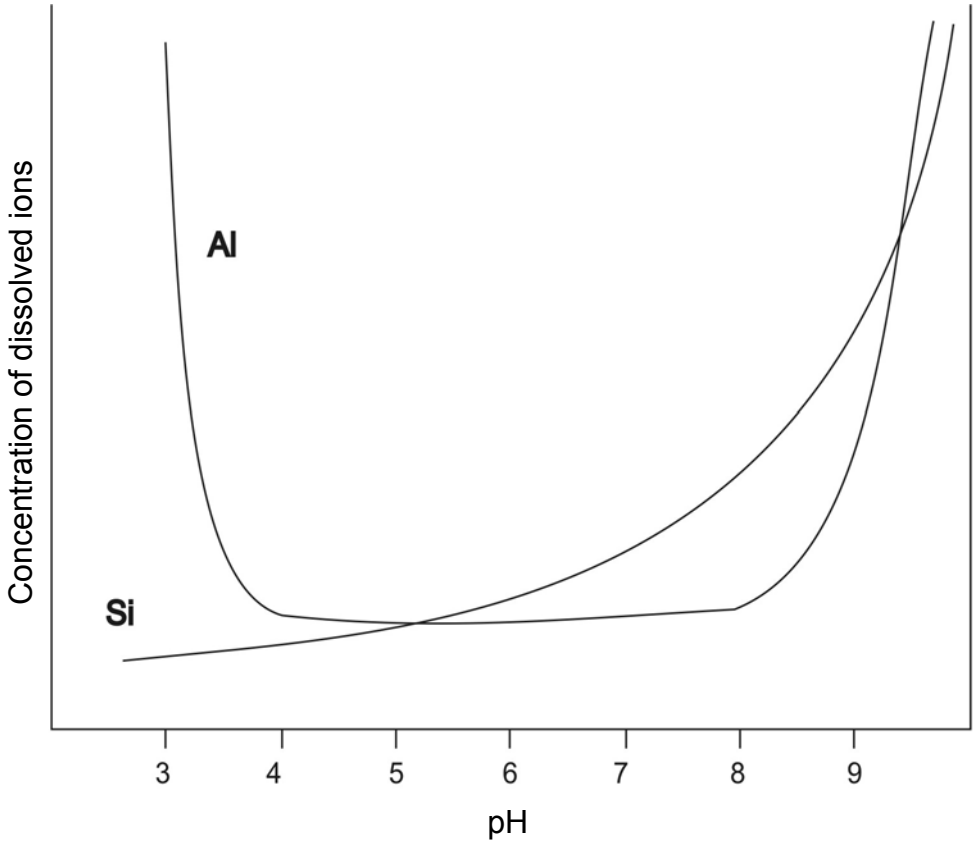

Figure 8.7: *Solubility of Si and Al minerals with varying pH (Bertolino, 2011).*

It is also interesting to note that at the start of accelerating creep for both LS7 and MS4, the pH values seem to stabilize. Whereas for MS4, there is a steady decline in pH until start of accelerated creep as seen on Fig. 7.12, the opposite is seen for LS7; where a steady increase prior to start of accelerated creep is observed, as seen from Fig. 7.5. One might argue that this is due to the different pH value of the injecting brine, and that it should be expected that the pH values in the effluent of LS7 would be higher than that of MS4. However, as seen from both Fig. 7.6 and 7.7, the pH values

in the effluent for both LS8 and LS9 are fluctuating around pH 7.6 – 7.8, even though the pH for the injecting brine for LS9 was much higher than that of LS8 (pH 10 and pH 6 for LS9 and LS8, respectively). A pH buffering process seems to be occurring in the same nature for both LS8, LS9 and MS4, where the chalk seems to buffer the pH to a value of approximately 7.6, regardless of the injecting brine. As this is not seen in LS7, it may suggest that the high pH values can be the result of the proposed dissolution of non-carbonate minerals.

It is also evident from the sudden change in pH development at start of accelerated creep for both MS4 and LS7, that there are in fact pH dependent chemical processes occurring during accelerated creep phase, and that these processes may differ somewhat for MS4 and LS7. Exactly what is occurring and how it is affecting the creep compaction is uncertain, however considering the opposite behaviours for LS7 and MS4, it may be due to the difference in magnesium concentration in the injecting brines, or the difference in purity of the outcrop chalks.

When considering Liège chalk cores, it has also been previously established that there is in fact a relationship between the concentration of magnesium present in the flooding brine and the resulting strain rate (Madland et. al., 2011). The strain rate was shown to increase with an increasing concentration of magnesium (see Fig. 8.8). According to the results from Madland et al. (2011), the final strain rate for LS7 would be expected to be in the vicinity of approximately 0.8 to 1.0%/decade, while the final strain rate for LS7 during the accelerated creep phase was in fact a magnitude of almost 2.4 to 3.0 times higher than this; 2.385%/decade. However, if calculating the strain rate prior to the accelerated creep phase, LS7 would in fact fit better with the correlation shown by Madland et al. (2011); with a strain rate of 0.69%/decade. The chalk cores presented in Fig. 8.8 did not experience the same accelerated creep phase as that of LS7, but nor were they flooded with a high pH brine. This discrepancy from the model further suggests that pH may have an impact on the accelerated creep phase experienced by LS7.

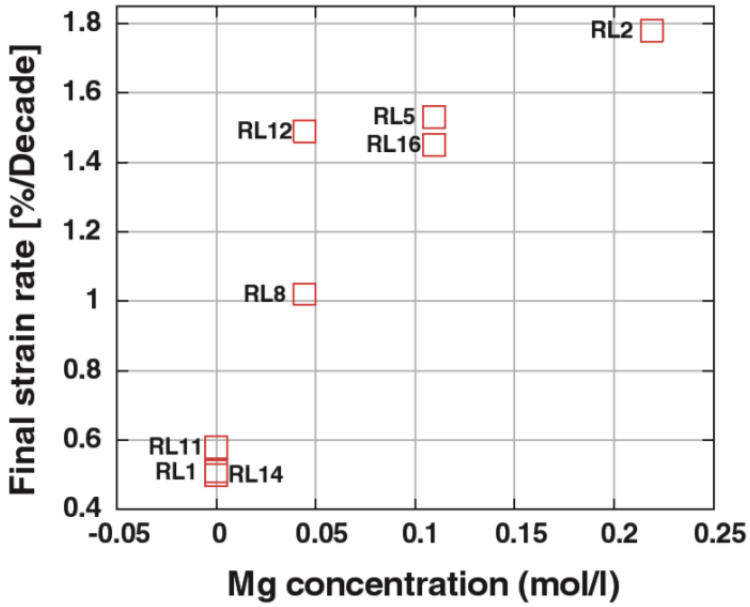

Figure 8.8: *Relationship between magnesium concentration in the flooding brine and the resulting final strain rates for Liège chalk cores (Madland et al., 2011).*

As seen in Fig. 8.9, it is clear that there is in fact a difference in the response to the chemical processes occurring in the cores of MS4 and LS7 during the accelerated creep phase. For MS4, there is a pronounced increase in both produced calcium from the chalk core and retained magnesium inside the chalk core at start of accelerating creep phase. This is not seen in LS7, where the amount of retained magnesium and produced calcium seem to suddenly stabilize at start of accelerated creep phase.

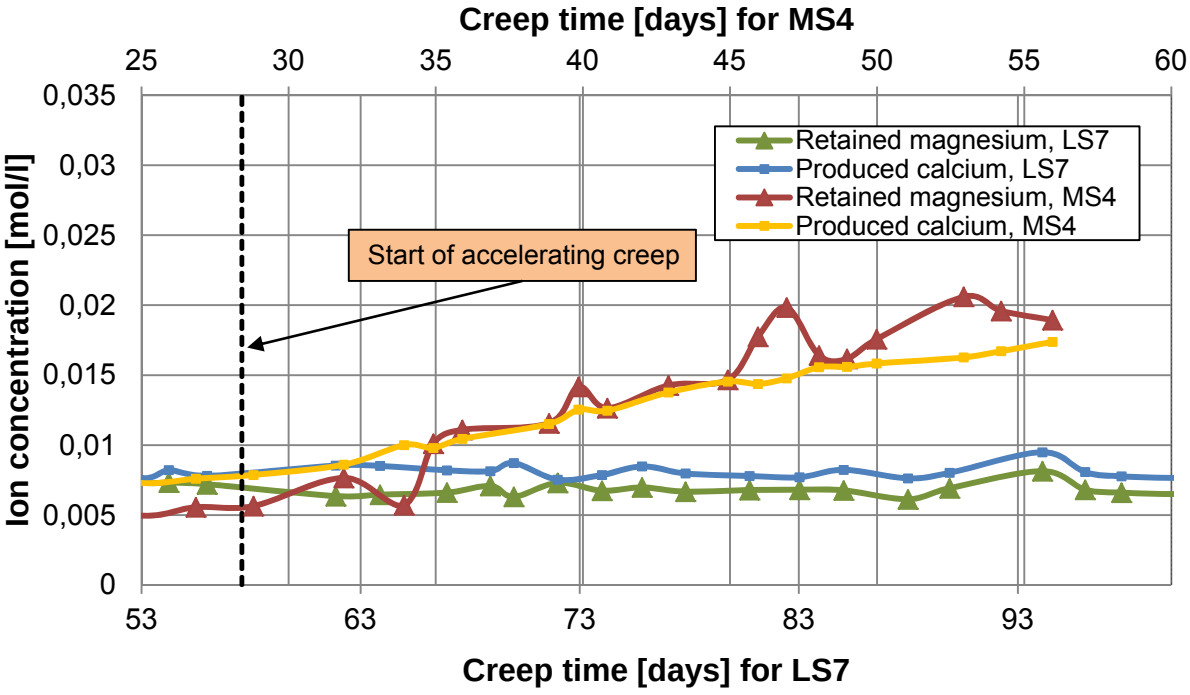

Figure 8.9: *Ion concentration of retained magnesium and produced calcium for both LS7 (lower X-axis) and MS4 (upper X-axis) from start of accelerating creep phase.*

8.2.4 Time delay effect

It is observed from Fig. 8.3 that the accelerated creep compaction does not occur instantly. There seem to be a time delay effect for both LS7 and MS4, where it requires 52 and 22 days, respectively, of magnesium flooding before any accelerated creep compaction is observed. At first sight, one might argue that this difference in time delay might be associated with the difference in magnesium concentration. However, Megawati et al, (2011) also reported a time delay of 40 days prior to an accelerated creep compaction of Liège chalk cores when flooding high pH 0.219M $MgCl_2$. This could suggest that the excessive time delay experienced in LS7 compared to MS4 might be associated with the pH dependent non-carbonate dissolution as discussed in chapter 8.3. The sole reason for the time delay experienced by both outcrop chalks is not fully understood. There is, however, reason to believe that there exists a relation between the purity of the chalk core and the magnitude of the time delay. Madland et al. (2011) reported that Stevns Klint chalk, which is an even more pure chalk than Mons but with equal porosity, only experienced a time delay of approximately 9 days when flooded with 0.219M $MgCl_2$.

The importance of the time frame for these experiments is demonstrated by these profound time delays, especially considering that LS7 needed 60 days of magnesium flooding prior to any initiation of accelerating creep phase. In previous studies, there has been little emphasis on the time frame of the experiments. In Madland et al. (2011), the time frame for experiments presented was merely between 5 and 20 days of creep time. Had these tests been allowed to creep even further, one may speculate that the results, especially considering the final strain rates, would have been different.

9 Conclusion

The importance of non-carbonate content and effect of alkaline brine flooding in chalk has been thoroughly investigated through both short and long term mechanical testing. Both the highly pure Mons chalk, with non-carbonate content of less than 0.3%, and the less pure Liège chalk, with non-carbonate content of approximately 5 %, has been flooded with both magnesium containing and non-magnesium containing brines. From the results of the tested Mons core, where an increase of magnesium was being retained inside the core and excessive calcium was being produced at start of accelerated creep, it is clear that the precipitation of secondary magnesium bearing minerals and dissolution of calcite may result in enhanced creep compaction as it has been shown previously (Madland et al., 2011; Megawati et al., 2011).

When considering magnesium ions as an important factor in the water weakening effect of chalk, there might be a correlation between magnesium concentration in the flooding brine and the resulting creep compaction. Although the 0.0445 M $MgCl_2$ flooded Liège core showed calcium production and magnesium retention during the accelerated creep, both concentrations stabilized during this phase rather than the increasing behavior shown by the results from both the 0.219M MgCl2 flooded Mons core from this study, and the 0.219M MgCl2 flooded Liège core presented by Megawati et al. (2011). This may further suggest that other chemical processes are accountable for the enhanced creep compaction. Considering the fairly high weight percentage of non-carbonate content to that of Liège chalk compared to Mons chalk, and the assumption that these non-carbonate minerals are filling the intergranular voids, the enhanced creep compaction can be the result of increased dissolution of non-carbonate minerals, causing a diminishing of the chalks intergranular contact points. It is also evident that the effect of alkaline flooding is only observed when flooding with magnesium containing brines, further demonstrating magnesium as the key ion to be aware of when considering the water weakening effect of chalk. However, the small magnesium concentration on the flooding brine of the tested Liège chalk may be the reason why this core did not experience the same creep compaction as that of the tested Mons core. This may point towards that the concentration of magnesium may in some cases override the effect of the presence of other non-carbonate minerals which has previously shown to contribute to an enhanced water-induced compaction. Thus it is not only the content of silicates and quarts that are of

importance, however, a sufficient amount of Mg^{2+} is also needed in order to cause enhanced creep.

Based on these great time delays, it is evident that long term testing is necessary in order to fully understand the processes of the water weakening effect on chalk. Especially when considering that the Liège core flooded with 0.0445 M $MgCl_2$ needed 60 days of flooding prior to the initiation of the accelerated creep phase. Further considering the relatively small total axial creep strain of this Liège core (compared to that of the tested Mons core), one may for example speculate if a second accelerated creep phase would have been initiated if the core had been tested even further.

10 References

Bertolino, S., 2011. Personal conversation.

Blanton, T.L., 1981. Deformation of Chalk Under Confining Pressure and Pore Pressure. *SPE 8076*, SPEJ, February

Darquennes, A., Vandycke, S., Schroeder, C., 2007. Deformation of faulted white chalk in Belgium. *GEOLOGICA BELGICA*, 10/3-4: 145-147.

DaSilva, F., Sarda, J.P., Schroeder, C., 1985. Mechanical behavior of chalks. *2nd North Sea Chalk Symposium, Book 2*, Stavanger, Norway.

Downs, H. H., Hoover, P. D., 1989. Enhanced oil recovery by wettability alteration. In: Oil-Field Chemistry. Enhanced recovery and production simulation. Eds. Borchardt J.K. and Yen, T. F., *ACS Symposium Series 396*. Washington D.C.

Fabricius et al., 2007. Modelling elastic properties of impure chalk from South Arne Field, Norsh Sea, *Geophysical Prospecting, v. 55*, p. 487-506

Farouq-Ali, S. M., Stahl, C. D., 1970. Increased oil recovery by improved waterflooding. *Earth and Mineral Sciences, Volume 39,* No. 4, January, pp. 25-28.

Fjær, E., Holt, R. M., Horsrud, P., Raaen, A. M., Risnes, R., 1991. Petroleum related rock mechanics. ISBN 0-444-88913-2

Hjuler, M., Fabricius, I.L., 2009. Engineering Properties of chalk related to diagenetic variations of Upper Cretaceous onshore and offshore chalk in the North Sea area. *Journal of Petroleum Science and Engineering 68*, pp 151-170

Hjuler, M., 2006. Silica and clay mineralogy and distribution in reservoir chalk (Valhall) and outcrop chalks (Stevns, Aalborg and Liège), *doctorial thesis*, University of Stavanger.

Korsnes, R.I., et al., 2008. Anisotropy in chalk studied by rock mechanics. *Journal of Petroleum Science and Engineering 62,* pp 28-35

Korsnes, R.I., 2007. Chemical induced water weakening of chalk by fluid-rock interactions, *doctorial thesis*, University of Stavanger.

Korsnes, R.I., et al., 2006a. Does the reaction between seawater and chalk affect the mechanical properties of chalk? *Eurock 2006, Multiphysics Coupling and Long Term Behaviour in Rock Mechanics- Cottheim, A.V., et. al*., London (2006), pp. 427-434. ISBN 0 415 41001 0.

Korsnes. R.I., et al., 2006b. Impact of Brine Composition on the Mechanical Strength of Chalk at high Temperature. *Eurock 2006, Multiphysics Coupling and Long Term Behaviour in Rock Mechanics- Cottheim, A.V., et. al.,* London (2006), pp. 427-434. ISBN 0 415 41001 0.

Lord, C.J., Johlman, C.,L. and Rhett, D.W., 1998, Is Capillary Suction a Viable Cohesive Mechanism in Chalk? *Eurock '98*, Trondheim, Norway

Madland, M.V., E. Omdal, Megawati, T. Hildebrand-Habel, R.I. Korsnes1, S. Evje, L.M. Cathles, A. Hiorth., 2011. Chemical alterations induced by rock–fluid interactions when injecting brines in high porosity chalks. *Transp. Porous Med.*

Madland, M.V., Midtgarden, K. Manafov, R. Korsnes, R.I. Kristiansen, T.G., Hiorth, A., 2008.The effect of temperature and brine composition on the mechanical strength of Kansas chalk. *International Symposium of the Society of Core Analysts*, Abu Dhabi, UAE, SCA2008-55, pp. 1–6

Madland, M.V., 2005. Water weakening of chalk – a mechanistic study, *doctorial thesis*, University of Stavanger.

Madland, M.V. and Risnes, R., 1999. Capillary effects in high porosity chalk. *2nd Euroconference on Rock Physics and Mechanics*. Edinburgh, Scotland, 14-18 November

Megawati, M, Andersen, P.Ø, Korsnes, R.I., Evje, S., Hiort, A., Madland, M.V. The effect of aqueous chemistry pH on time-dependent deformational behaviour of chalk - experimental and modeling study. *Flows and mechanics in natural porous media from pore to field scale. Pore2Field*, IFP Energies nouvelles, Paris, November 16-18, 2011

Miller, J.P., 1952. A portion of the system calcium carbonate-carbon dioxide-water, with geological implications. Am J Sci 250:161–203

Moller, N., Christov, C., and Weare, J., 2006. Thermodynamic models of aluminium silicate mineral solubility for application to enhanced geothermal system, *Thirty-First Workshop on Geothermal Reservoir Engineering: Stanford University*, Stanford, California

Newman, G.H., 1983. The effect of water chemistry on the laboratory compression and permeability characteristics of some North Sea Chalks*. J. Petroleum technology 35*, pp. 976-980.

Richard, J., Sizun, J,-P. (2011) Pressure solution-fracturing interactions in weakly cohesive carbonate sediments and rocks: Example of the synsedimentary deformation of the Campanian chalk from the Mons Basin (Belgium). *Journal of Structural Geology 33*, pp154-168

Richard, J., Sizun, J,-P., Machhour, L., 2005. Environmental and diagenetic records from a new reference section for the Boreal realm: The Campanian chalk of the Mons basin (Belgium). *Sedimentary Geology*, 178: 99-111.

Risnes, R., 2001. Deformation and Yield in High Porosity Outcrop Chalk. *Phys. Chem. Earth (A). Vol 26*, NO 1-2, pp 53-57.

Risnes, R., Haghighi, H., Korsnes, R.I., Natvik, O., 2003. Chalk-fluid interactions with glycol and brines. *Tectonophysics 370*, 213-226.

Roelh, P.O., Choquette, P.W. (Editors), 1985. Carbonate Petroleum Reservoirs. *Springer-Verlag*, New York, pp 622.

Schmoker, J.W., Krystinik, K.B., Halley, R.B., 1985. Selected characteristics of limestone and dolomite reservoirs in the United States. *Bull. Am. Assoc. Prerol. Geologists*, 69: 733-741

Scroeder, C., Bois, A.-P., Maury, V. and Halle, G., 1998. Water/Chalk (or collapsible soil) interaction: Part II. Results of test performed in laboratory on Lixhe chalk to calibrate water/chalk models, *Eurock '98*, Trondheim, Norway

Spencer, A.M., Briskeby, P.I., Christensen, L.D., Foyn, R., Kjølleberg, M., Kvadsheim, E., Knight, I., Larsen, M.R., Williams, J., 2008. Petroleum geoscience in Norden – exploration, production and organization. Episodes, 31, 115-124

Sylte, J.E., Thomas, L.K., Rhett, D.W., Bruining, D. D., Nagel, N. B., 1999. Water induced Compaction and the Ekofisk Field, *SPE Annual Technical Conference and Exhibition*, Houston, Texas. United States of America

Vorland, K.A.N., 2004. The influence of seawater injection on the mechanical strength of chalk, *master thesis*, University of Stavanger.

White, W.B., Scheets, B.E., and Silsbee, R., 1998, Interaction of aqueous metal silicates with mine water, *Tailings and Mine waste*, Balkema, Rotterdam.

Zenger, D.H., Dunham, J.B., Ethington, R.L., 1980. Concepts and models of dolomitization. *Spec. Publ.-SEPM 28*, pp 320

Zhang, X., Salemans, J., Peach, C.J., Spiers, C.K., 2002. Compaction experiments on wet calcite powder at room temperature: evidence for operation of intergranular pressure solution. *Deformation Mechanisms, Rheology and Tectonics: Current Status and Future Perspectives.* Geological Society, London, Special Publications, 200, pp 29-39